Environment International 163 (2022) 107189

Contents lists available at ScienceDirect

Environment International

journal homepage: www.elsevier.com/locate/envint

Full length article

Estimation of RF and ELF dose by anatomical location in the brain from wireless phones in the MOBI-Kids study

Carolina Calderón [a,*], Gemma Castaño-Vinyals [b,c,d,e], Myron Maslanyj [a], Joe Wiart [f,g], Ae-Kyoung Lee [h], Masao Taki [i], Kanako Wake [j], Alex Abert [b,c,d], Francesc Badia [b,c,d,k], Abdelhamid Hadjem [f], Hans Kromhout [l], Patricia de Llobet [b,c,d], Nadège Varsier [f], Emmanuelle Conil [f,m], Hyung-Do Choi [h], Malcolm R. Sim [n], Elisabeth Cardis [b,c,d]

[a] UK Health Security Agency, Chemical, Radiation and Environmental Hazards, Chilton, Didcot, Oxon OX11 0RQ, United Kingdom
[b] Barcelona Institute of Global Health (ISGlobal), 88 Doctor Aiguader, E-08003 Barcelona, Spain
[c] University Pompeu Fabra, Barcelona, Spain
[d] CIBER Epidemiologia y Salud Pública, Madrid, Spain
[e] IMIM (Hospital del Mar Medical Research Institute), Barcelona, Spain
[f] WHIST Lab Common Lab of Orange Labs R&D and Institut Mines Telecom, Issy-les-Moulineaux, France
[g] LTCI, Telecom Paris, Institut Polytechnique de Paris, 91120 Palaiseau, France
[h] Radio Technology Research Department, Electronics and Telecommunications Research Institute (ETRI), Yuseong-gu, Daejeon, Korea
[i] Department of Electrical Engineering, Graduate School of Engineering, Tokyo Metropolitan University, Japan
[j] Electromagnetic Compatibility Laboratory, Electromagnetic Standards Research Center, Radio Research Institute, National Institute of Information and Communications Technology, Koganei, Japan
[k] University Autónoma de Barcelona, Spain
[l] Institute for Risk Assessment Sciences (IRAS), Utrecht University, Utrecht, the Netherlands
[m] Agence Nationale des FRéquences (ANFR), Maisons-Alfort, France[1]
[n] School of Public Health and Preventive Medicine, Faculty of Medicine, Nursing and Health Science. Monash University, Alfred Centre, Commercial Road, Melbourne, Victoria 3004, Australia

ARTICLE INFO

Handling Editor: Adrian Covaci

Keywords:
ELF-EMF
RF-EMF
Mobile phones
Dose algorithm
Exposure assessment
Brain tumour

ABSTRACT

Wireless phones (both mobile and cordless) emit not only radiofrequency (RF) electromagnetic fields (EMF) but also extremely low frequency (ELF) magnetic fields, both of which should be considered in epidemiological studies of the possible adverse health effects of use of such devices. This paper describes a unique algorithm, developed for the multinational case-control MOBI-Kids study, that estimates the cumulative specific energy (CSE) and the cumulative induced current density (CICD) in the brain from RF and ELF fields, respectively, for each subject in the study (aged 10–24 years old). Factors such as age, tumour location, self-reported phone models and usage patterns (laterality, call frequency/duration and hands-free use) were considered, as was the prevalence of different communication systems over time.

Median CSE and CICD were substantially higher in GSM than 3G systems and varied considerably with location in the brain. Agreement between RF CSE and mobile phone use variables was moderate to null, depending on the communication system. Agreement between mobile phone use variables and ELF CICD was

Abbreviations: AMPS, Advanced Mobile Phone System; APC, Adaptive Power Control; CDMA, Code-Division Multiple Access; CICD, Cumulative Induced Current Density; CSE, Cumulative Specific Energy; DECT, Digital Enhanced Cordless Telecommunications; DTx, Discontinuous Transmission; EDGE, Enhanced Data rates for GSM Evolution; ELF, Extremely Low Frequency; EMF, Electromagnetic Fields; FDTD, Finite-Difference Time-Domain; GSM, Global System for Mobile communications; HFK, Hands-free kit; HSPA, High Speed Packet Access; IARC, International Agency for Research on Cancer; ICD, Induced Current Density; IDEN, Integrated Digital Enhanced Network; LTE, Long-Term Evolution; MRI, Magnetic Resonance Imaging; NBT, Neuro-epithelial Brain Tumours; PDC, Personal Digital Cellular; PHS, Personal Handyphone System; RF, radiofrequency; SAR, Specific Absorption Rate; SMSP, software modified smartphone; TBW, Total Body Water; TDMA, Time Division Multiple Access; TMA900, Telefonía Móvil Automática (Automatic Mobile Telephony service); UMTS, Universal Mobile Telecommunications System; VoIP, Voice over Internet Protocol.

* Corresponding author at: UK Health Security Agency, Chemical, Radiation and Environmental Hazards, Chilton, Didcot, Oxon OX11 0RQ, United Kingdom.
E-mail address: carolina.calderon@ukhsa.gov.uk (C. Calderón).
[1] Present affiliation.

https://doi.org/10.1016/j.envint.2022.107189
Received 21 December 2021; Received in revised form 28 February 2022; Accepted 14 March 2022
0160-4120/Crown Copyright © 2022 Published by Elsevier Ltd. This is an open access article under the CC BY-NC-ND license (http://creativecommons.org/licenses/by-nc-nd/4.0/).

higher overall but also strongly dependent on communication system. Despite ELF dose distribution across the brain being more diffuse than that of RF, high correlation was observed between RF and ELF dose.

The algorithm was used to systematically estimate the localised RF and ELF doses in the brain from wireless phones, which were found to be strongly dependent on location and communication system. Analysis of cartographies showed high correlation across phone models and across ages, however diagonal agreement between these cartographies suggest these factors do affect dose distribution to some level. Overall, duration and number of calls may not be adequate proxies of dose, particularly as communication systems available for voice calls tend to become more complex with time.

1. Introduction

Mobile phones are held close to the head during conversations, and as a result some of the energy from the radiofrequency (RF) electromagnetic fields (EMFs) emitted by phones is absorbed by the brain. This has led to concerns that there may be long-term health effects, such as brain tumours, linked to mobile phone use. Most of the epidemiological studies that investigated possible adverse health effects from mobile phones have used proxies, such as self-reported duration and number of calls, to quantify EMF exposure to the brain. INTERPHONE was the first epidemiological study to examine possible health effects from mobile phones based on individual dose estimates (the cumulative specific RF energy (CSE) absorbed) at the location of the tumour as opposed to using cumulative call time as proxy for exposure. The study found that, in the adult brain, most of the RF energy from mobile phones was absorbed in the outer surface of the temporal lobe, on the side of the head where the phone was used, and misclassification was non-negligible when using call time as opposed to CSE (Cardis et al., 2011a).

In addition to RF, mobile phones also emit extremely low frequency (ELF) magnetic fields (Calderón et al., 2014; Calderón et al., 2017; Gosselin et al. 2013) which induce currents in the brain, but this type of exposure has yet to be included in mobile phone epidemiological studies. Indeed, ELF was mentioned as a possible confounder of the association between RF and brain tumour risk in INTERPHONE (Cardis et al. 2011a).

MOBI-Kids is a subsequent case-control multi-national epidemiological study that investigated the possible association of brain tumours and exposure to wireless phones – both mobile and cordless, including exposure to RF and ELF EMFs in children and young adults (Castaño-Vinyals, 2022; Sadetzki et al., 2014). It advances the previous epidemiological research by also including ELF exposure and focuses on effects of exposure in childhood and adolescence, a subject of concern in recent years due to the growing use of mobile communication technologies in young people.

This paper presents the algorithm that was designed to estimate the lifetime dose – specifically CSE for RF exposure and cumulative induced current density (CICD) for ELF exposure – for each subject in MOBI-Kids who reported use of mobile or cordless phones. This work builds on the

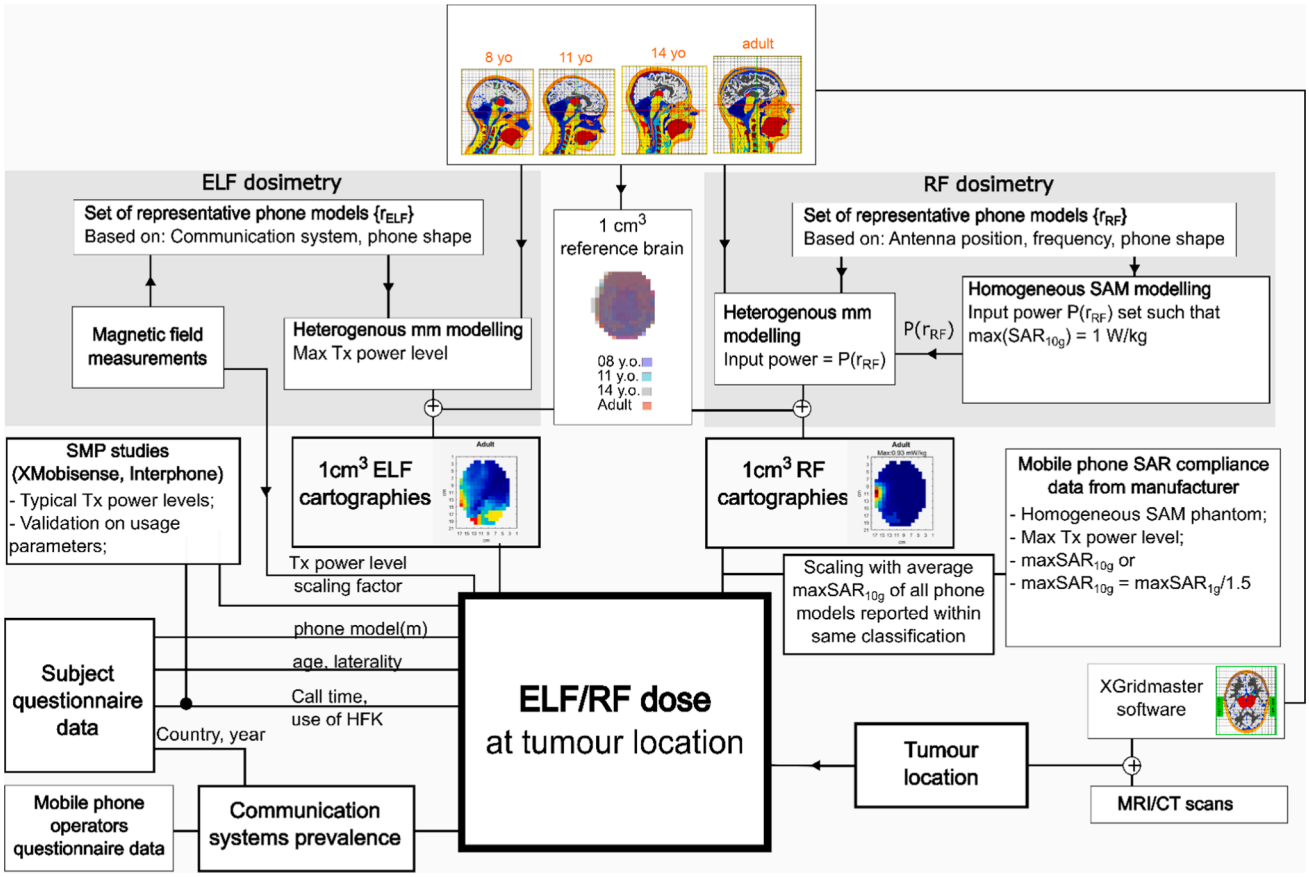

Fig. 1. ELF and RF algorithm for MOBI-Kids for mobile phone exposure. Algorithm for Digital Enhanced Cordless Telecommunications (DECT) phones is similar. Appendix A The variable SAR_{1g} and SAR_{10g} refers to the localised SAR averaged over 1 g and 10 g of contiguous tissue, respectively. The maximum SAR_{1g} and SAR_{10g} over the brain is labelled in the figure as $maxSAR_{1g}$ and $maxSAR_{10g}$.

INTERPHONE algorithm (Cardis et al., 2011b), by also taking into account ELF EMFs, recent improvements in dosimetry and the evolution of communication systems over the last two decades, some of which have been shown to result in differences in both RF and ELF dose by an order of magnitude or greater (Calderón et al., 2017; Wiart, 2013). Refinements were also possible as a result of the MOBI-Expo validation study, complementary to MOBI-Kids, which utilised an app to validate mobile phone use reported by young people (Goedhart et al., 2018). Doses were estimated for all mobile or cordless phone users in the study across the 14 participating countries, and a statistical analysis was performed to determine the level of agreement between dose and self-reported use of mobile phone, and between RF and ELF dose.

2. Materials and methods

2.1. Main elements of RF and ELF dose algorithms

The main structural elements of the RF and ELF dose algorithm are shown schematically in Fig. 1 and the following subsections describe the different sources of information that were used to construct the algorithm.

2.1.1. Information on usage from MOBI-Kids study subjects

Between 2011 and 2015, subjects in the study were interviewed to ascertain their mobile phone usage and exposure to possible confounders such as ionising radiation and pesticides, as well as medical history. Each subject responded to a face-to-face questionnaire in the local language administered by a trained interviewer, except for a small percentage where the interview was done over the phone – 4% of cases and 6% of controls (Castaño-Vinyals et al., 2022). Those who were regular users of mobile phones (defined as making or receiving calls at least once a week for a period of 3 months or more) were asked a series of questions related to their mobile phone use during their lifetime. The questions were used to quantify various exposure variables: number and length of calls (making/receiving); mobile phone operators used; use in urban vs rural areas; laterality and hands-free use (HF, which includes use of hands-free kit and speaker mode), in particular use of Bluetooth headsets as this was deemed to be a potential additional source of RF/ELF to consider. Similarly, subjects were asked about usage of cordless phones (laterality, number/duration of calls, use of HF).

Study participants were also asked to report the different models of mobile phones they used. A catalogue, with over 7000 phone models marketed between 2000 and 2015 in the participating countries, was created to help subjects identify the model. Information in the catalogue included make and model, year of commercialisation, phone type (including shape and position of external antenna where available), communication systems supported, connectivity, and other phone characteristics (e.g. battery, voltage and Specific Absorption Rate (SAR)), where available. When a subject did not remember the exact phone model that they had used, prompts were used (classic vs. special shaped; flip vs. slide vs. neither; smartphone; visible antenna; functionalities) to try to allocate the phone into one of the a priori constructed phone categories (discussed in Section 2.1.3). If no information was available, even after prompts (6% of total number of phones reported), the phone model was imputed based on the most popular phone used in that country and that year.

Voice calls made over Wi-Fi using Voice over Internet Protocol (VoIP) with mobile phone applications such as Skype and WhatsApp are a low-cost alternative to network calls and thus were also considered in the questionnaire. However, data from the MOBI-Kids questionnaire showed that only 19% of participants reported using VoIP, and the amount of use was very low during the period of interest, with a median of less than 8 min per day. Moreover, these applications are typically used for video calls, where the phone is located far from the head during use, resulting in negligible EMF exposure to the brain. For these reasons VoIP was not included in the algorithm.

Information was also gathered on text messaging and uploading data (e-mail, browsing the internet), though again it was not included in the algorithm on the basis that these services usually involve using the phone away from the head.

2.1.2. Input from validation studies

Dose at any given location in the brain will depend on whether the phone was being held close to the head and if so, on which side (laterality). As part of MOBI-Kids, a validation study (MOBI-Expo) was undertaken to characterise and validate mobile phone use habits in young people (Goedhart et al., 2018). Results were used to inform the various answers in the MOBI-Kids questionnaire. Information such as laterality, duration of calls and hands-free use was recorded by an Android application developed by WHIST Lab (X-Mobisense) and compared with reported mobile phone use. Results from 466 participants across the 12 participating countries (Australia, Canada, France, Germany, Greece, Israel, Italy, Japan, Korea, New Zealand, Spain and the Netherlands) showed that laterality was much more evenly distributed than previously assigned, with self-reported right-side users holding the phone on the right side for about 70% of the time (as opposed to the 90% value assigned in INTERPHONE (Cardis et al., 2011b)) and self-reported left-side users holding the phone on the left side for around 50% of the time. Subjects with no preferred laterality were found to use their phone on the right side for around 60% of the time, similar to that assigned in INTERPHONE (50%).

Hands-free use was categorised into ‘Almost never or rarely’, ‘Less than half the time’ and ‘Half the time or more’ for both mobile phone and cordless phones (asked separately). In INTERPHONE these categories translated to 0%, 25% and 75% of use respectively. However, Mobi-Expo revealed that these proportions were much lower in the age range of subjects in MOBI-Kids, translating to 3.5%, 7% and 18.5% respectively for headset and speaker use (for both mobile phones and cordless phones), and 0%, 1% and 10% respectively for Bluetooth specifically (Goedhart et al., 2018).

2.1.3. Phone categories

The EMF exposure from a mobile phone at any given time will depend on various factors. For RF, exposure is dependent on the design of the device (i.e. phone model), the frequency used by the communication system, the power input to the transmitting antenna, and the position of the phone with respect to the head (distance to the head, laterality, orientation).

Most of these parameters can also have an impact on ELF exposure, but, unlike RF, frequency band is not a main determinant of ELF exposure, but communication system frame structure is (Calderón et al., 2017). Frame structure determines the temporal pattern of the phone transmissions which will affect the waveform (temporal pattern) of the electrical current being drawn from the battery, which gives rise to the ELF magnetic fields.

It was unfeasible to model the induced current density (ICD) and SAR for all phone in the catalogue. Also, many mobile phone designs were very similar. Thus, a set of RF and ELF phone classifications were defined based on an assessment of the most popular phone models and on various exposure determinants found through the measurements and computational modelling performed as part of the study (Calderón et al., 2017; Lee et al., 2017; Lee et al., 2016).

For RF, five main generic categories of phones were developed and modelled, based on their shape: bar phones (small screen, physical keypad), smartphones (large screen, no keypad), flip phones with internal and external antenna, and slide phones. For flip phones with internal antenna and for slide phones, subclasses were also investigated to account for differences in the antenna location (top/hinge, bottom) and, in the case of slide phones, in usage configuration (opened, closed). An averaging process was used to derive representative ICD and SAR distributions (referred to as cartographies) for these two categories. Thus, for flip phones, the average of the cartographies with the antenna at the

Table 1
Communication systems included in the algorithm together with their maximum output powers, scaling factors for conversion to typical power levels, and duty factors. For introduction of each communication system, see Appendix A.

Communication system	*Handset frequency bands, MHz*	*Approximate period used (country dependent)*	*Participating countries that reported having deployed this technology (from operator data)*	*Maximum emitted power (W)*	*Duty factor*	*Maximum averaged emitted power (W)*	*Scaling factor for typical output power for RF A_{APC}*	*Reference*
GSM	900 1800	1991– Present	All participating countries except Japan/ South Korea	2 1	0.125 0.125	2*0.125 = 0.25 0.125	0.5 0.5	(Vrijheid et al. 2009)
UMTS	900 1700 2000	2001– Present	All participating countries	0.25	1	0.25	Urban 0.0067 Rural 0.0133	(Gati et al. 2009)
CDMAOne	800 1900	1995–2000	South Korea/Canada/ Israel	0.2	1	0.2	0.005	(Kelsh et al. 2011; Lee and Choi 2020)
CDMA2000	800 1900 2100	2000 – Present	South Korea/Canada/ Israel	0.2	1	0.2	0.005	
PDC	900 1500	1991 – 2012	Japan	0.8	1/3 (full rate) 1/6 (half-rate)	0.8*0.28 = 0.22	0.5	(Wake et al., 2005)
PHS	1900	1995–2020	Japan	0.08	1/8	0.01	1	
DECT	900 1500	1992 – Present	ALL	0.25	1/24	0.25	1[a]	

[a] While a form of APC is available on recent DECT phones (eco DECT), it was deemed not to be prevalent during the period of interest for the study.

top and at the hinge was used. For slide phones, the average of the cartographies with the antenna at the top and bottom was used to calculate average cartographies for open and closed configurations. A weighted average was then used to calculate the overall set of cartographies, which assumed phone calls were made 75% of the time with the slide phone opened, and 25% of the time closed. For the bar phone model, the antenna was assumed to be on the top of the phone, and for the smartphone it was assumed to be at the bottom of the phone. South Korea was able to obtain information on antenna location for each phone model reported, thus specific subclass cartographies were used accordingly. Most South Korean bar phone models had the antenna at the bottom, so these were classified as smartphones instead.

The antennas of all modelled phones were designed to emit at (or close to) the frequencies used by the communication systems across the various participating countries, namely in the 800–900 MHz band (low frequency band) and the 1750 MHz–1950 MHz band (high frequency band). The mobile communication systems included in the algorithm, along with their prevalence (based on Section 3.3) and other operational characteristics are shown in Table 1, and brief definitions of the communication systems are provided in Appendix A. Communication systems used for data and not widely used for voice calls, such as Enhanced Data rates for Global System for Mobile communications Evolution (EDGE) and High-Speed Packet Access (HSPA), were not included in the algorithm.

In terms of ELF, communication systems which use Time Division Multiple Access (TDMA) schemes (such as GSM, PHS, PDC, and DECT), transmit in periodic bursts, and the frequency components of the ELF magnetic field are dictated by the frequency of the transmission bursts (Appendix A). On the other hand, for communication systems which use Code Division Multiple Access (CDMA) schemes, transmission is constant throughout the call and variations in current and thus magnetic field are small, and spectral profile is noisier (Calderón et al., 2017). In terms of spatial distribution, the ELF magnetic field from a mobile phone can be modelled as a small loop, and the position of this loop has been observed to be within the boundaries of the phone's battery (Calderón et al., 2014; Gosselin et al., 2013). Information on battery position was not readily available in the catalogue, but in the sample of GSM and UMTS phones assessed within the study, flip/slide phones were found to have, on average, a lower battery position than bar phones, by around 3 cm (Calderón et al., 2014). Thus, it was possible to classify phones based on their communication system, and in the case of GSM and UMTS, the phone shape (bar phones versus flip/slide phones).

Cordless phones were assumed to be Digital Enhanced Cordless Telecommunications (DECT) phones as this was the standard for cordless phones in most participating countries since the late 1990s (Stüber, 2017). For RF, a specific larger bar phone was designed to represent the DECT phone. For ELF, modelling was based on specific measurements made over a small sample of DECT phones (Calderón et al., 2017).

Results from preliminary investigations on Bluetooth exposure from an earpiece showed that both RF and ELF exposure from Bluetooth devices was likely to be negligible and hence use of Bluetooth hands-free kit (HFK) was treated the same as any other HFK.

2.1.4. Computational dosimetry

The accurate calculation of the SAR induced by RF sources and ICD induced by ELF sources requires realistic numerical models of the human body, also known as phantoms. Adult and child phantoms have been intensively studied using mathematical, voxelized or synthetic methods (Christ et al., 2010; Dimbylow, 1995; Lee et al., 2009; Lee et al., 2006; Nagaoka et al., 2004; Wiart et al., 2008; Wu et al., 2011; Xu and Eckerman, 2009). Even though the brain reaches its adult size (shape and volume) after about 5 years (Courchesne et al., 2000; Han et al., 2018; Lee et al., 2019; Wiart et al., 2008), the pinna, skin, skull thickness and the lower part of the head continue to evolve with age, and the same RF source can therefore result in different doses if used at different ages. It was therefore important for the study to assess the brain dose at different stages of development. Taking into account the different organs' development over time, the age of the study subjects and the available child head phantoms, four different head models were chosen from the Virtual Population set of phantoms, developed by IT'IS (Christ et al., 2010; Gosselin et al., 2014), representing an 8-year-old (Eartha), 11-year-old (Billie), 14-year-old (Louis) and an adult (Duke) (Fig. 1, Fig. S1). These are heterogeneous models, containing 13 different brain

Table 2
Main ELF frequencies for the various communication systems included in the algorithm.

Communication system	Main ELF frequency, Hz	Relative amplitude with respect to GSM ICD (maximum 1 cm^3 ICD)[2]
GSM	217	1
UMTS	Variable (typically 100)	0.04
CDMAOne	90[1]	0.02[1]
CDMA2000	90	0.02
PDC	50	0.07
DECT	100	0.09
PHS	200	0.008

[1] Same values as CDMA2000 were used, based on communication system similarities in frame structure and output power.
[2] Comparisons from numerical modelling, at maximum power level.

tissues[2] with a resolution of 1 mm. Adult dielectric properties were used for all phantoms, as the dielectric properties of tissues are likely to differ little in the age range covered by MOBI-Kids (Gabriel et al., 1996a; Wang et al., 2006). This is supported by empirical calculations (Wang et al., 2006) and by analyses of the influence of the dielectric properties of tissues (based on the TBW - Total Body Water) on whole body averaged SAR where differences of 5.8%, 3.6%, and 2.5% were observed for a 1-, 3-, and 5-year-old respectively (Lee and Choi, 2012). RF calculations were performed using the Finite Difference Time Domain (FDTD) numerical method and ELF calculations were performed using the impedance method (Orcutt and Gandhi, 1988).

2.1.4.1. RF. The input power to the transmitting antenna is a key parameter in the computational modelling of the phones and depends on the power emitted by the RF amplifier in the frequency band of interest, as well as possible losses/mismatches in the link between the antenna and the amplifier, which are specific to each handset. However, all mobile phones on the market are required by law, e.g. the Radio Equipment Directive (RED) in Europe (2014/53/EU 2014) or previously the Radio equipment and Telecommunications Terminal Equipment Directive (1999/5/EC, 1999), to provide maximum SAR measurements averaged over 10 g or 1 g of tissues ($maxSAR_{10g}$ or $maxSAR_{1g}$). These measurements follow well-defined international standards, such as the IEC 62209–1528 standard (IEC-62209-1528, 2020). SAR is linearly proportional to input power, and thus the latter can be used as a proxy for SAR. Hence, a reference input power, P_{ref}, was defined such that it would result in a maximum SAR_{10g} of 1 W/kg when using a specific anthropomorphic mannequin (SAM) phantom and the phone in the 'cheek' position, as defined by the IEC 62209 standard. This reference input power $P_{ref}(c)$ was defined for each of the phone categories, labelled c, and subsequently used for the detailed numerical modelling with the four heterogeneous head models. Then, once all phone model information was gathered from the participants, the modelling was scaled to the average $maxSAR_{10g}$ for each phone category. This was the average across all models reported in a given category and for which there was $maxSAR_{10g}$ or $maxSAR_{1g}$ data available. If only maximum SAR over 1 g was provided by manufacturers, a scaling factor, $CF = 1.5$, was applied to convert to a SAR over 10 g, where $maxSAR_{10g} = maxSAR_{1g}/CF$ (Lee et al., 2018). The scaling with average $maxSAR_{10g}$ includes the reduction in power from frame structure duty factors in Time Division Multiple Access (TDMA) systems.

The IEC 62209–1528 standard (IEC-62209-1528, 2020) specifies "Cheek" and "Tilt" mobile phone positions. However, phone position is likely to vary during a call, across calls, and across subjects. Several studies, based on numerical and advanced stochastic methods were performed to analyse the influence of the handset position on brain RF dose (Ghanmi, 2013; Ghanmi et al., 2014). These studies showed that the RF SAR distribution in the brain can be approximated by using five positions: the "Cheek" and "Tilt" positions, with the angles {θ,φ} respectively equal {0°,0°} and {15°,0°}, and 3 additional positions: {25°,0°}, {8°,+10°}, {8°,-10°}, where θ is the tilt angle between phone and cheek and φ is the rotational angle about the axis connecting both ears (Fig. S2). In the absence of information on handset position and to account for the likely variation in this parameter, the average of the SAR distributions across all five different phone positions was used for each of the categories. In all cases, an equal probability for each position was assumed.

2.1.4.2. ELF. ICD modelling was performed for various communication systems (GSM, UMTS, CDMA2000, PDC, DECT). Cartographies were also made available separately for bar phones and flip/slide phones for GSM and UMTS, based on magnetic field measurements of samples of phones using these communication systems. The results of this work, published elsewhere (Calderón et al., 2014; Calderón et al., 2017), were used as inputs to the algorithm presented here. Unlike with RF, only 'cheek' position was assumed during modelling, which was considered the worst-case scenario. The frequencies used for the ELF numerical modelling (and dielectric properties) are specified in Table 2. As the magnetic field waveform from mobile phones comprises several frequency components, the original models were scaled to allow for them, as described in Calderon et al. (Calderón et al., 2017).

Use of CDMAOne has practically faded come to an end since 2001, therefore there were no phones and equipment available to perform measurements. However, due to the similarities in frame structure between CDMA2000 and CDMAOne, CDMA2000 was used as a proxy for CDMAOne. In the same way, due to similarities in magnetic field distribution, DECT phones were used as proxy for PHS phones, albeit with a scaling factor that reflected the differences in output power and frequency composition. The relative amplitude between the various communication systems, derived by comparing maximum ICDs in the cartographies, is shown Table 2.

2.1.5. Tumour location and cartographies

A program called Gridmaster was developed in the INTERPHONE study to allow neuroradiologists to define the location of a tumour within the computational head phantom used for the dosimetry on the basis of diagnostic scans (Cardis et al., 2011b). The program displayed coronal, sagittal and transverse outlines of the phantom. Since tumour localisation is a complex process, relying heavily on the experience of the neuroradiologist, it is done at centimetre resolution. Thus, the high-resolution dosimetry calculations were projected over a superimposed grid of 1 cm^3 resolution.

Large advances in phantom models since the development of the Gridmaster allowed the creation of an improved version of the program for this study (XGridmaster), with added anatomical information as a function of age (Fig. S1). Thus, the homogeneous head model of the original program was replaced with the four heterogeneous head models, mentioned above. The neuroradiologists were able to use the most relevant phantom for comparison with the diagnostic scan (Magnetic Resonance Imaging or Computed Tomography scan if the former was not available) and select all the 1 cm^3 voxels of the tumour in the corresponding phantom, using the various tissue structures in the underlying high resolution brain as references for more accurate location. The centre of gravity (COG) was subsequently calculated as the geometric centre of the total volume of the tumour.

To transfer the high-resolution modelling onto the 1 cm^3 coordinate system of the XGridmaster, the edges of the high-resolution brain were aligned with the orthogonal axes of the XGridmaster, and dose

[2] Grey matter, White matter, Cerebellum, Commissura anterior, Commissura posterior, Hippocampus, Hypophysis, Hypothalamus, Medulla oblongata, Midbrain, Pineal body, Pons and Thalamus.

distributions (SAR or ICD) were averaged within each superimposed 1 cm^3 voxel of the XGridmaster. Because the size of the brain is not a multiple of a centimetre, some 1 cm^3 cubes were only partially filled by 1 mm^3 cubes. These have been kept for the purpose of the study, and the same averaging method was used for these cubes. The voxels concerned were mainly located on the opposite side of the head where the phone was placed, where the RF and ELF dose was estimated to be very low.

Although anatomical changes in the brain do occur after 6 years of age, brain volume is not expected to change materially (Giedd et al., 2006; Wiart et al., 2011). However, due to anatomical variabilities within the general population, brain volume varied (non-monotonically) across the particular phantoms used. Thus, to help determine dose at the tumour location as a function of age, a reference brain was defined, which encompassed the volume of the four phantom brains (Fig. S1, Fig. 1). Cubes with missing data (due to imperfect overlapping between the original brain and the reference brain) were assigned the maximum 1 cm^3-averaged value from the closest cubes with data. The brain models were overlapped in such a way as to minimise extrapolation in the areas of highest RF and ELF dose (see section c in Fig. S2). The resulting 1 cm^3 averaged maps are the final maps used for determining dose at the tumour location and referred to as cartographies.

2.1.6. Typical transmitting power from phones

The RF cartographies were scaled to the average $maxSAR_\{10g\}$maximum SAR over 10 g reported by mobile phone manufacturers, which is measured when the phone is transmitting at highest power level, for exposure compliance testing purposes. However, except for PHS phones, mobile phones adapt their transmitting power in order to minimise interference with other users and to maximise battery life, a process known as adaptive power control (APC). Thus, to scale the cartographies to typical power levels, a factor, labelled hereafter A_{APC}, was included in the algorithm to take account of this reduction in power. SAR is linearly dependent on the RF transmission power, and thus typical power levels reported in the scientific literature can be used directly to scale the cartographies. It should be noted that this scaling is related to typical power levels, and as such is independent of any reduction in exposure due to the duty factors from TDMA frame structure, which was included in the scaling of the cartographies with $maxSAR_{10g}$.

For RF, the values for $A_{APC,RF}$ for the various communication systems are shown in Table 1. Some of these values were derived from work done for INTERPHONE as the same communication systems had been used (Cardis et al., 2011b; Vrijheid et al., 2009; Wiart et al., 2000). For UMTS, typical power levels depend on whether the call was made in a rural or urban environment (Mahfouz et al., 2012), and the total scaling factor was thus described by $A_{APC,RF}(UMTS) = A_{urban,UMTS}\cdot\tau_{urban} + A_{rural,UMTS}\cdot\tau_{rural}$, where τ_{urban} and τ_{rural} represent the proportion of time calls were made in rural and urban environments respectively, as specified by participants in the questionnaire, and $A_{urban,UMTS}$ and $A_{rural,UMTS}$ are the scaling factors for urban and rural areas respectively (Table 1, (Mahfouz et al., 2012)).

For ELF with pulsed RF transmissions such as GSM and PDC (i.e. TDMA systems, see Appendix A), magnetic fields, and thus the ICD, are also dependent on transmission power. However the relation is not linear as it is related to the current drawn from the battery (Calderón et al., 2017), not the power. Based on magnetic field measurements as a function of transmission power level and the fact that modelling was done at maximum power level, $A_{APC,ELF}$ was found to be equal to 0.75, 1 and 0.9 for GSM1800, GSM900 and PDC respectively (Calderón et al., 2014; Taki, Personal communication). For UMTS, CDMAOne and CDMA2000, ELF exposure is effectively independent of power level. This is because transmission is not pulsed (i.e. power level affects the continuous (static) current level rather than the ELF components), and because of the efficient power management techniques used (Calderón et al., 2017). Thus, for ELF $A_{APC,ELF}(s) = 1$ for $s = \{UMTS, CDMA, CDMAOne\}$.

2.1.7. Discontinuous Transmission, DTx

In order to reduce power consumption and interference, Discontinuous Transmission (DTx) is used during GSM and PDC voice calls (Wiart et al., 2000), whereby the phone pauses transmission during silent periods. In INTERPHONE this led to a reduction in RF duty factor of 30% for GSM (Cardis et al., 2011b). The same factor was applied for the algorithm described here. In ELF, the current density induced by a magnetic field depends on the rate of change of the magnetic flux density waveform (dB/dt), thus mainly on the rise of TDMA bursts, and DTx is not expected to have a material influence. In terms of spectral changes due to DTx, these were found to result in changes of about 10% in ICD (for a reduction of duty factor of 30%), and thus DTx was not included.

2.1.8. Prevalence of communication systems

The time-weighted average power at maximum power level is similar for GSM 900, UMTS, CDMA and DECT, but the differences in typical power levels between the various mobile communication systems (i.e. APC scaling) result in GSM RF exposures being around 50 times larger than UMTS and CDMA at the same frequency (Table 1), while in ELF, GSM 900 ICD can be 25 times larger than that of UMTS (second column in Table 2). Thus, it was important to know the proportion of time a given communication system was used during a voice call. As this information was unavailable, it was necessary to make assumptions. For this, operators in each participating country were sent a questionnaire to obtain a list of all communication systems (and frequency bands) used for voice calls since the year 2000 (information prior to this was available from a similar questionnaire in INTERPHONE), together with dates of deployment and termination of use, where applicable. For communication systems (or frequency bands) that saw a decline in prevalence since 2000, maximum proportion of voice traffic, and the date when the proportion started to decline were also asked.

Linear interpolations and extrapolations were made with the information collected (complemented with operator data from the INTERPHONE study), to evaluate the fraction of time, $Traffic_{voice}(s,t,o)$, a communication system was used for voice calls at time t and for operator o (hereafter, s denotes both communication system and frequency band, e.g. GSM900, GSM1800): If operators started using GSM 900 before GSM 1800 (e.g. Spain, operator A in Fig. 4), GSM900 was assumed to be the only communication system used until GSM1800 started, and then GSM 900 was decreased linearly over time and GSM1800 simultaneously increased to reach the proportion reported in the questionnaire at the time UMTS was introduced (taken as 60:40 if not specified). From that time, GSM900 and GSM1800 were assumed to decrease linearly in parallel while UMTS increased linearly to reach the proportion reported at the time of the questionnaire (2015). If not provided, this was taken to be 57% GSM and 43% UMTS (the average over all operators with data at that time). If operators started using GSM 1800 before GSM 900 (e.g. Spain, operator B in Fig. 4), then the reverse was done for GSM proportions. For countries without any data (Austria, France, New Zealand), mean proportions were calculated using the data from other operators and countries.

At the end of the period of interest, in 2015, 75% of UMTS traffic was assumed to be in the 2100 MHz frequency band and 25% in the 900 MHz frequency band for all operators using both, based on the limited information obtained.

Not all phones had the latest capabilities offered by their network. Therefore, for each phone reported,p, the contribution to exposure from communication system s was only included if the phone model in question had the capability of using that system; denoted by the binary variable $X(model(p),s)$:

$$P_{voice}(s,t,p) = \frac{X(model(p),s)\cdot Traffic_{voice}(s,t,o(p))}{\sum_{s'} X(model(p),s')\cdot Traffic_{voice}(s',t,o(p))} \quad (1)$$

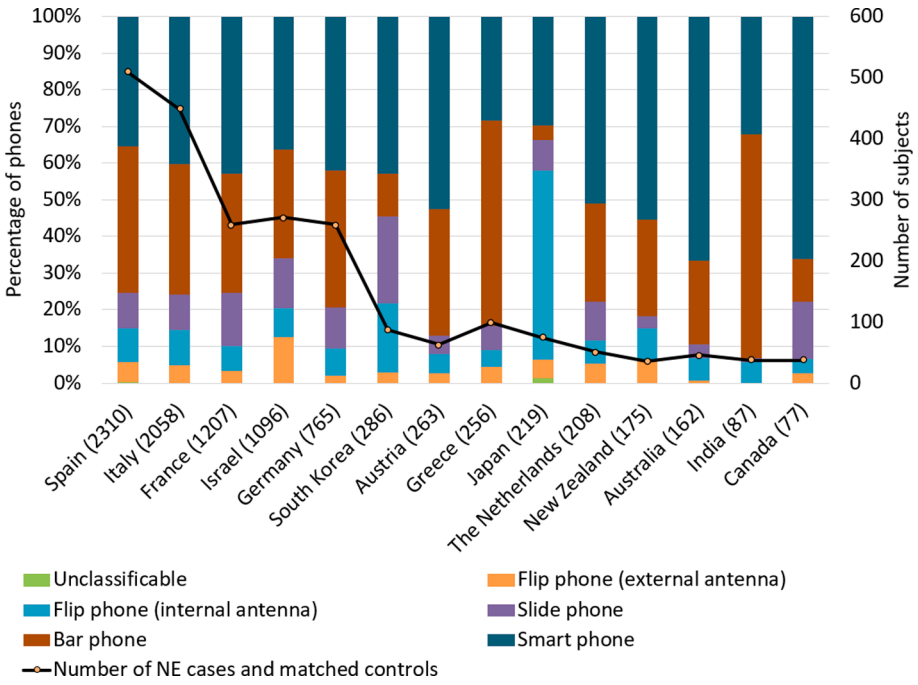

Fig. 2. Distribution of phones reported by the MOBI-Kids neuroepithelial (NE) cases, and matched controls, by phone class and geographical area. Countries are in order of number of phones reported for that country, shown in brackets. Typically, subjects reported having used more than one phone, and thus the total number of phones is greater than the total number of subjects.

where $o(p)$ is the operator for mobile phone p as reported by the subject. The capabilities of the phones were ideally obtained from the phone model specifications, although information about phone capability was requested in the questionnaire when the study subjects did not remember the phone model used.

Information on prevalence of communication systems was also used, together with reported mobile phone use, to determine the number of subjects who had used each communication system considered in the study.

2.2. The RF and ELF dose algorithm

The various elements of the RF and ELF algorithm for the MOBI-Kids study are summarised schematically in Fig. 1. For the purposes of the study and based on the source and exposure considerations discussed in the previous sections, the RF and ELF 'dose' at voxel v of the reference brain arising from the use of a mobile phone in communication system and frequency s is described by the $CICD_s$, in A•hours/m^2 ($Dose_s = CICD_s$), and the CSE_s, in J/kg ($Dose_s = CSE_s$), respectively, both of which can be described as a combination of usage and intrinsic dose:

$$Dose_s = \sum_{i=1}^{N_{months}} \sum_{k=1}^{2} \sum_{p=1}^{N_i^{phones}} Usage(i,k,p) \cdot Exposure(s,i,k,p,v) \quad (2)$$

Where N_{months} was the number of months of phone usage, N_i^{phones} is the number of mobile phones reported at month i, and $k = 1$ or 2 for left or right laterality respectively. The contribution of usage to the dose estimate was given by:

$$Usage(i,k,p) = T_i \cdot \alpha_X \cdot \tau_k^{lat}(l_i) \cdot \left(1 - \tau_i^{HF}\right) \cdot \tau_p^{phone} \quad (3)$$

Where T_i is the total reported duration of calls over month i (in hours), α_X is a factor which converts T_i to the required units ($\alpha_{RF} = 3600 \frac{seconds}{hour}$, $\alpha_{ELF} = 1$) $\tau_k^{lat}(l_i)$ is the proportion of time exposure is assigned to laterality k given reported laterality l_i for month i, τ_i^{HF} is the proportion of time hands-free use was reported for month i, and τ_p^{phone} is the proportion of time phone p was used at month i, set to $1/N_i^{phone}$.

The intrinsic dose from mobile phones was given by:

$$Exposure(s,i,k,p,v) = P_{voice}(s,t_i,p) \cdot M(h(i),c(p),s,k,v) \cdot A_{APC,X}(s) \cdot DTx(s) \quad (4)$$

Where $P_{voice,p}(s,t_i,p)$ is the proportion of communication system s used for voice calls at time t_i for operator of phone p, as defined in Eqn. (1). $M(h(i),c(p),s,k,v)$ is the dose at voxel v (SAR for RF and ICD for ELF) for communication system s, phone classification $c(p)$ of phone p, head $h(i)$, and laterality k. The scaling to take into account typical power levels, $A_{APC,X}(s)$ was described above, where $X = \{RF,ELF\}$, and the DTx scaling $DTx(s) = 1$ except for RF and for $s = \{GSM900, GSM1800, PDC\}$ where it was set to 0.7.

The algorithm for DECT was a simplified version of the one used for network calls:

$$Dose_{DECT} = \sum_{i=1}^{N_{months}} T_i^{DECT} \cdot \alpha_X \cdot \left(1 - \tau_i^{HF,DECT}\right) \sum_{k=0}^{1} \tau_k^{lat,DECT}(l_i) \cdot M(DECT,h(i),k,v) \quad (5)$$

The total CICD and total CSE was given by summing over all communication systems (and frequency bands) considered (including DECT).

Although not discussed in detail here, time weighted average induced current density (TWAICD) over defined time windows was also considered as an alternative metric in the risk analysis and was calculated straightforwardly from the above equations.

2.3. Statistical analysis

The algorithm described above was used to estimate RF and ELF doses for all 2041 subjects in the MOBI-Kids study who reported having used wireless phones. Dose was estimated at the centre of gravity (COG) of the tumour for the neuro-epithelial brain tumour cases whose tumour location was determined by a neuroradiologist, and the same location was assigned for their matched controls.

As in INTERPHONE (Cardis et al., 2011b), the level of agreement between RF and ELF dose versus mobile phone use variables (call time, number of calls), as well as between ELF dose and RF dose (i.e. CICD

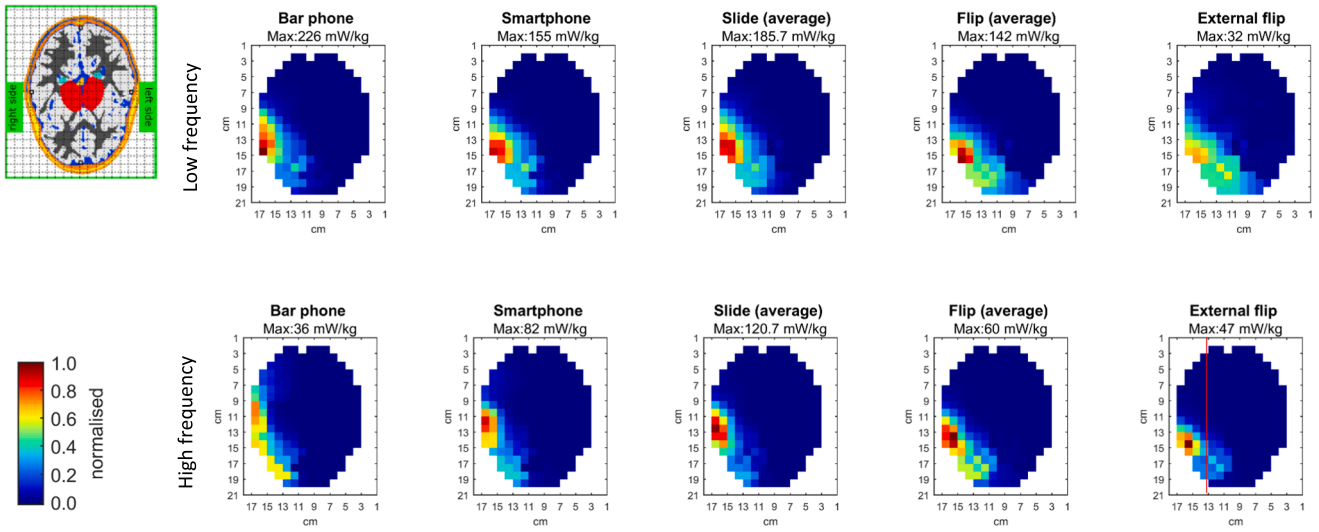

Fig. 3. Top view (horizontal cut) of RF SAR spatial distribution by frequency (top row: low frequency band, bottom row: high frequency band) and phone type, for adult head phantom. First figure on the left shows the phantom in the XGridmaster, for reference. The plots are normalised to the highest 1 cm^3 SAR across the whole brain (shown in subtitles), which may not necessarily be in the slice shown here. The red line on the bottom right image is the cut shown in Fig. S3. (For interpretation of the references to colour in this figure legend, the reader is referred to the web version of this article.)

versus CSE) was estimated using Cohen's weighted Kappa (κ_w) coefficient, comparing deciles of the distribution of the variables. A linear weight was used (Cohen, 1960; Cohen, 1968). The percentage of agreement on the diagonal, defined as the proportion of cells where the decile classification of dose and of the use variable coincided, was also calculated. The Cohen's weighted Kappa (κ_w) coefficient was also calculated to compare terciles between dose (ELF or RF) and time since start of wireless phone use. For this calculation the weights were defined as: full agreement weight on the diagonal, 0.5 for adjacent cells to the diagonal and zero otherwise.

A similar analysis was also performed to compare the level of agreement between SAR cartographies (across phone categories and across ages). That is, if for a given cell, dose in one cartography fell in the same decile of another cartography. This effectively compares the level of agreement of the SAR distribution normalised to its maximum. Pearson correlation was also calculated for the comparison between cartographies, as well as for the comparison between RF and ELF dose as these were quantities on a continuous scale. These statistical analyses were conducted in R programme (version 3.6.3) and Matlab (Cardillo, 2007).

3. Results

3.1. Phone categories

Fig. 2 shows the distribution of phones reported by study subjects by phone category across all participating countries. A total of 9169 phones were reported by NE cases and controls. Overall, almost three quarters of phone models reported were either smart phones (40%) or bar phones (34%), and in the case of India, these accounted for over 93% of the 87 phones reported. The exception was Japan, where flip phones were more prevalent than smartphones.

The average $maxSAR_{10g}$ values, used to scale the maps as described in Section 2.1.4, were found to be similar across phone categories: 0.67 W/kg for smartphones (N = 1387, SD = 0.20 W/kg), 0.68 W/kg for bar phones (N = 664, SD = 0.24 W/kg), 0.57 W/kg for slide phones (N = 519, SD = 0.24 W/kg), 0.72 W/kg for flip phones with internal antenna (N = 377, SD = 0.29 W/kg), and 0.75 W/kg for flip phones with external antenna (N = 45, SD = 0.23 W/kg).

3.2. Cartographies and comparison between various communication systems

Spatial RF SAR distributions across the brain are shown, by phone category and frequency band, in Fig. 3 and Fig. S3 for the adult brain. The corresponding SAR distribution for DECT phones is shown in Fig. S4, together with the ELF ICD distributions. The corresponding SAR distributions by age group and phone category are provided in Figs. S4 – S9.

As expected, SAR distributions were very localised. The exact location of the maxima differed across phone classifications, and when SAR values were grouped into deciles, mean diagonal agreement was 33% and 32% for low and high frequency respectively, and mean weighted kappa was 0.63 and 0.61 respectively. However, mean correlation between the smartphone cartography and the other phone classification cartographies (while keeping age and frequency constant) was 0.90 and 0.80 for low and high frequency respectively (Table S1). Despite differences in antenna location, the bar phone and smart phone had similar SAR distributions (Fig. 3) with a mean correlation of 0.91 across heads and frequency bands (Table S1), albeit a mean diagonal agreement of 35% (range: 33%–39%) and a mean kappa of 0.67 (range: 0.65–0.71). An example contingency table, between bar phone and smartphone, for low frequency and adult phantom, is shown in Table S2 to illustrate how deciles from these two cartographies coincide. The average slide phone cartographies were also similar to the smartphone cartographies, with a mean correlation of 0.96 (range: 0.91–0.99), but a mean diagonal agreement of 41% (range: 32%–46%) and a mean kappa of 0.74 (range: 0.65–0.78). These three categories (smartphone, bar phone and slide phone) account for 85% of phones reported. Flip phone (internal and external antenna) show more differences with the other phone categories, when looking across the various ages (Figure S3 and Table S1). Correlation between DECT cartographies and smartphone cartographies (high frequency) ranged between 0.80 and 0.89 (across heads), while weighted kappa ranged between 0.57 and 0.65 and diagonal agreement ranged between 25% and 29%.

Comparing the adult head cartographies with the ones for the younger heads (while keeping phone category and frequency constant), yielded a mean Pearson correlation of 0.85 (range: 0.69–0.95) and 0.80 (range: 0.71–0.88) for the low and high frequency band respectively, where the mean was calculated across all phone categories and heads (Table S3). Mean observed diagonal agreement was 37% (range: 25%–

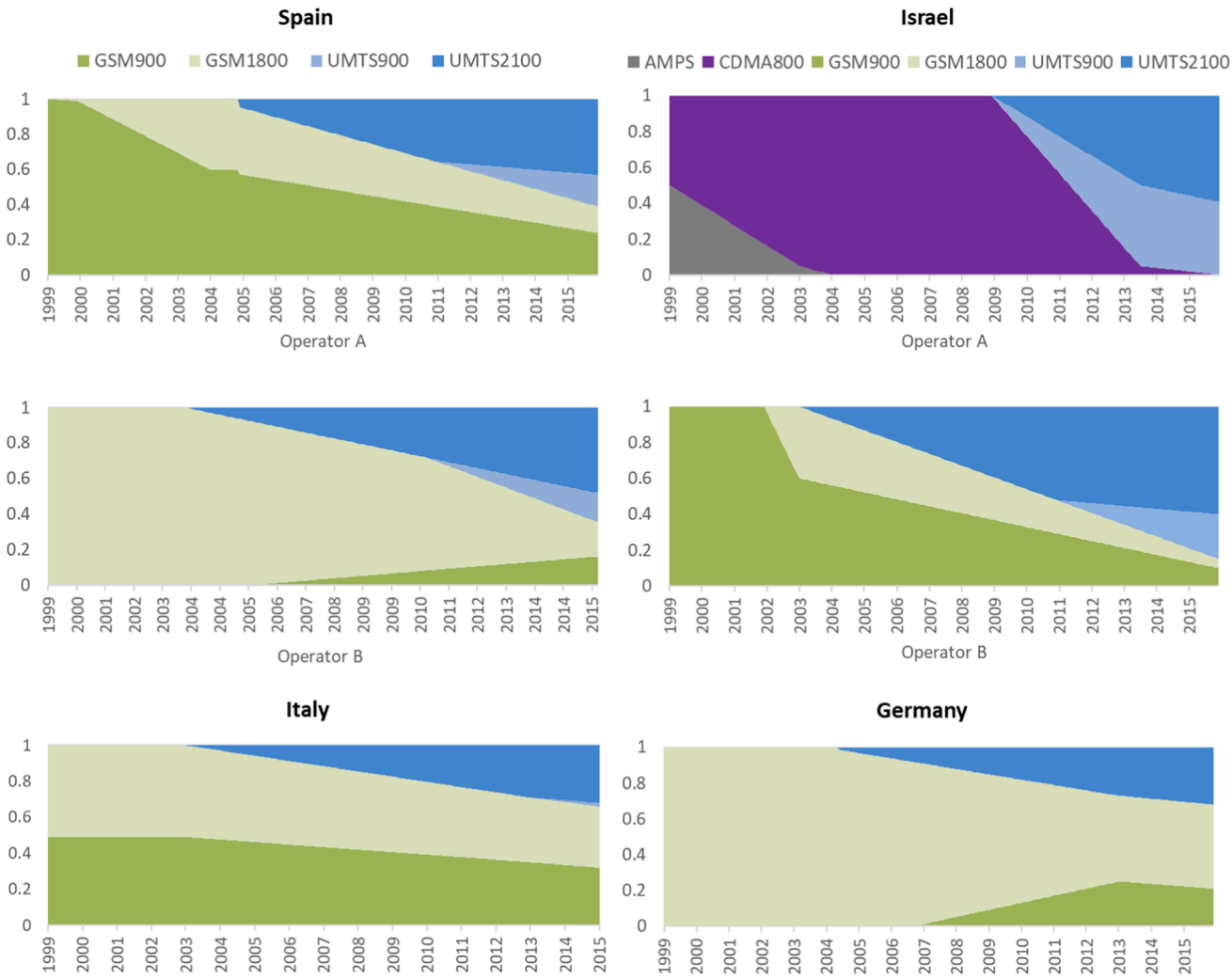

Fig. 4. Prevalence of communication systems across Spain, Israel, Italy and Germany.

52%) in the low frequency band, and 37% (range: 27% –47%) in the high frequency band, while mean kappa was 0.68 (range: 0.53–0.81) in the low frequency band and 0.71 (0.61–0.79) in the high frequency band. Agreement with the adult head increased with age for all phone categories in the high frequency band, but only for the flip (external antenna) phone at the low frequency band. Correlation values did not increase with age.

For ELF, ICD distributions for CDMA2000/CDMAOne, PDC and DECT had high kappa/correlation with the GSM/UMTS slide/flip phones (Table S4), most likely due to the lower position of the battery in the phone models used (CDMA2000 and PDC models were flip phones) (Table S4). Mean correlation between these cartographies and those of the slide/flip phones cartographies varied between 0.87 and 0.95, with a mean of 0.91 (mean diagonal agreement: 43%, 33%–62% weighted kappa: 0.77, 0.71–0.86). The cartography for GSM bar phones, on the other hand, had a mean correlation of 0.77 with the slide/flip phones and a range of 0.74–0.79 (mean diagonal agreement: 17%, 16%–19%, mean weighted kappa: 0.49, 0.46–0.51). Similar values were observed for the UMTS bar phone. In terms of effect of age, child cartographies had a mean correlation of 0.82 (0.77–0.86) with the adult head and across phone categories and different head phantoms, a mean agreement of 34% (26%–43%) and a mean weighted kappa of 0.67 (0.60–0.75, Table S4). No increase in observed agreement nor correlation was observed as a function of age.

ICD distributions were found to be more diffuse than SAR distributions (Fig. S4–5), with some ICD dose observed in the contralateral side (Calderón et al., 2017). When comparing ICD cartographies for GSM bar phones and SAR cartographies for bar phones in the high frequency band, the correlation varied between 0.70 (11-year-old) and 0.79 (adult), with a range in diagonal agreement of 23% (8-year-old and adult) and 26% (14-year-old), and a range in weighted kappa of 0.45–0.56. Similar values were observed when comparing the bar phone cartographies in the low frequency band. For DECT cartographies, the correlation ranged between 0.44 (14-year-old) and 0.55 (adult), with a diagonal agreement ranging between 14% (8-year-old) and 17% (11- and 14-year-old), and a range in weighted kappa of 0.23–0.38.

3.3. *Prevalence of communication systems*

Data from at least one operator was received for 11 out of 14 participating countries, with 5 countries providing information for several operators. All countries in the study which provided operator data reported having used GSM at some point between 1995 and 2015, except for South Korea and Japan. South Korea used CDMAOne (International Standard 95) in the mid-nineties until the introduction of CDMA2000 in the early 2000s (Lee and Choi, 2020), while Japan used PDC and CDMAOne. In terms of 3G systems, all countries in the study which provided operator data also reported having used UMTS. Canada and Israel also reported having used CDMA. Other communication systems, spanning from 1G to 4G, were reported by some operators (TMA900, AMPS, IDEN, VoLTE), but these were found not to be relevant to the study, either because: subjects did not report using phones at that

Table 3
Results of dose estimation for study subjects: estimated CSE absorbed at the centre of gravity of the tumour in J/kg[2], by communication system.

Communication system and frequency band	Number of subjects[1]	CSE, J/kg						
		Mean	Median	SD	Min	Max	25th quartile	75th quartile
Total mobile	2041	1625.40	132.91	7182.22	<0.01	199428.12	14.83	779.22
GSM 900	1608	1528.96	156.17	6550.78	0.01	160095.64	30.71	782.57
GSM 1800	1614	444.15	45.18	1688.12	<0.01	39310.05	7.99	248.46
UMTS 900	903	3.16	0.09	14.47	<0.01	218.02	0.01	0.76
UMTS 1800	75	11.66	1.24	46.33	<0.01	351.76	0.42	5.10
UMTS 2100	1351	3.44	0.35	14.36	<0.01	304.13	0.07	1.76
CDMA 800	247	44.30	7.11	160.27	0.02	2215.33	1.70	27.63
CDMA 1900	53	4.42	0.62	12.38	<0.01	85.00	0.13	2.96
PDC 1500	54	1690.47	84.89	4692.78	2.85	27091.69	23.52	381.58
DECT	1460	22.11	3.28	85.28	<0.01	1897.37	0.80	13.03

[1] Individual participants have generally used more than one communication system and frequency band over their wireless phone use history.
[2] In the epidemiological analyses, the RF dose was calculated using duration in hours instead of seconds.

Table 4
Results of dose estimation for study subjects: estimated CICD at the centre of gravity of the tumour in μA·hours/m^2, by communication system.

Communication system and frequency band	Number of subjects[1]	CICD (μA·hours/m^2)						
		Mean	Median	SD	Min	Max	25th quartile	75th quartile
Total mobile	2041	485.49	66.02	1372.13	0.002	19066.13	9.36	341.81
GSM 900	1608 (79%)	269.00	44.21	769.81	0.015	14384.34	8.03	197.02
GSM 1800	1614 (79%)	297.37	47.88	856.43	0.007	15590.72	7.45	213.28
UMTS 900	903 (44%)	1.18	0.06	5.75	<0.001	116.92	0.01	0.34
UMTS 1800	75 (4%)	5.59	1.97	10.68	0.003	62.33	0.74	5.45
UMTS 2100	1351 (66%)	4.62	0.70	15.33	<0.001	356.67	0.14	2.84
CDMA 800	247 (12%)	7.26	1.55	16.30	0.006	184.53	0.41	6.74
CDMA 1900	53 (3%)	4.03	0.71	9.93	0.002	62.89	0.22	3.12
PDC 1500	54 (3%)	21.02	0.80	73.74	0.023	487.06	0.34	5.55
DECT	1460 (72%)	44.47	8.12	124.12	0.038	2426.23	2.21	32.70

[1] Individual participants have generally used more than one communication system and frequency band over their wireless phone use history.

Table 5
RF TCSE at the centre of gravity of the tumour (in J/kg) vs mobile phone use variables.

		Number of calls											Duration of calls, hours										
		4 - 300	300 - 750	750 - 1300	1300 - 2100	2100 - 3200	3200 - 4800	4800 - 7000	7000 - 11000	11000 - 20000	20000 - 180000	Total	0,067 - 12	(12) - 32	32 - 62	62 - 110	110 - 180	180 - 300	300 - 510	510 - 890	890 - 1800	1800 - 33000	Total
TCSE, in J/kg	<2	89	54	15	21	9	8	2	3	0	2	**203**	93	55	41	8	3	3	0	1	0	0	**204**
	2 - 8	42	32	29	29	28	19	10	10	5	0	**204**	42	36	36	31	39	12	7	0	1	0	**204**
	8 - 24	33	34	38	20	24	14	18	8	9	5	**203**	37	38	22	30	20	26	15	11	5	0	**204**
	24 - 61	20	32	32	34	29	23	15	10	6	3	**204**	20	37	36	40	22	15	14	14	6	0	**204**
	61 - 133	11	18	41	24	22	29	22	20	10	7	**204**	8	20	33	42	26	23	22	16	10	4	**204**
	133 - 256	6	11	19	30	34	27	35	22	12	8	**204**	3	11	20	27	42	35	30	18	12	6	**204**
	256 - 540	1	11	15	14	16	29	30	36	27	25	**204**	1	4	12	15	24	33	38	44	24	9	**204**
	540 - 1188	2	4	6	18	18	27	19	36	46	28	**204**	0	3	1	6	19	33	41	42	45	14	**204**
	1188 - 3276	0	8	5	10	12	16	31	28	46	48	**204**	0	0	3	5	8	18	27	39	44	60	**204**
	3276 - 201600	0	0	4	4	11	12	22	31	43	78	**205**	0	0	0	0	1	6	10	19	57	112	**205**
	Total	**204**	**204**	**204**	**204**	**203**	**204**	**204**	**204**	**204**	**204**	**2039**	**204**	**204**	**204**	**204**	**204**	**204**	**204**	**204**	**204**	**205**	**2041**
											Weighted Kappa:	0.45									Weighted Kappa:	0.55
											% of agreement (diagonal only, dark grey cells):	21%									% of agreement (diagonal only, dark grey cells):	24%
											% of agreement (1 decile difference, light grey cells):	30%									% of agreement (1 decile difference, light grey cells):	35%
											% of agreement (2 decile difference):	21%									% of agreement (2 decile difference):	21%
											% of agreement (> 2 decile difference):	28%									% of agreement (> 2 decile difference):	20%

time and with the relevant operator; the phone model used was not compatible with the communication system in question; or the communication system was available after the censored date for subjects (1 year before reference date, which was the date of diagnosis for cases). Also, for the period of interest (except for a very short period in 1999), mobile phones using some of these communication systems (e.g. IDEN, PHS, PDC) could only use one system and thus proportion of network use for these systems would have been one. For these phones, phone model information would specify whether the communication system was used by subjects.

The prevalence of the communication systems reported by operators, for the four countries with the highest number of subjects (Spain: 23%,

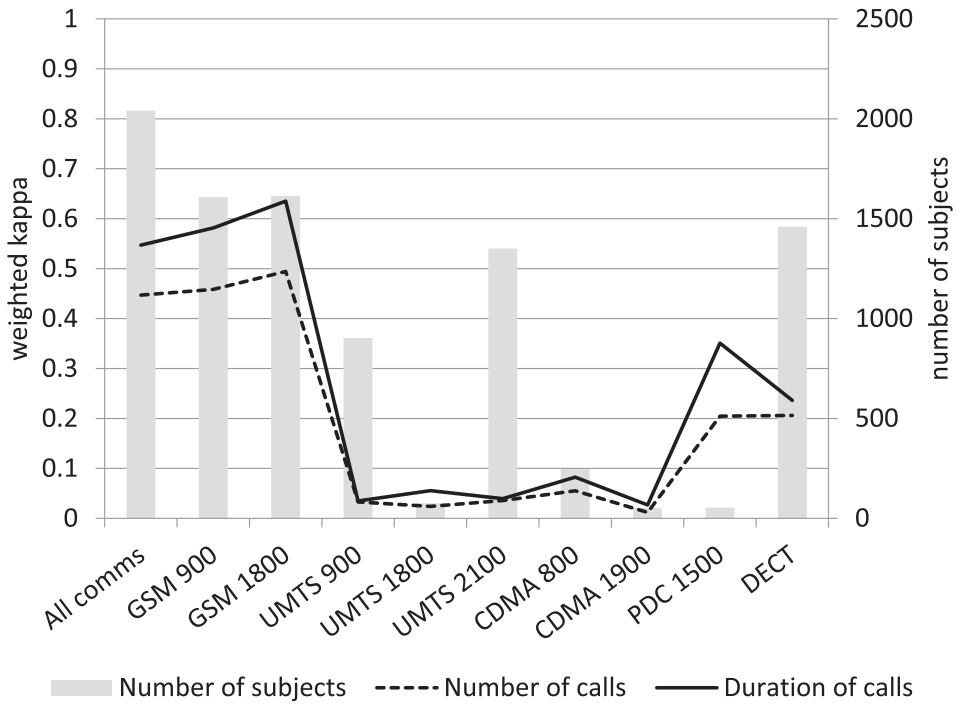

Fig. 5. Weighted kappa (and number of subjects) between CSE and cumulative call time and cumulative number of calls or the various communication systems and total RF dose.

Table 6
ELF TCID at the centre of gravity of the tumour (in μA·hours/m^2) vs mobile phone use variables.

		Number of calls											Duration of calls, hours									
		4 - 300	300 - 750	750 - 1300	1300 - 2100	2100 - 3200	3200 - 4800	4800 - 7000	7000 - 11000	11000 - 20000	20000 - 180000	Total	0,067 - 12	(12) - 32	32 - 62	62 - 110	110 - 180	180 - 300	300 - 510	510 - 890	890 - 1800	1800 - 33000	Total
TCID, in μA·hours/m^2	0.002 - 2.0	104	47	21	9	9	6	3	1	2	1	**203**	123	57	16	2	3	1	1	1	0	0	**204**
	2.0 - 6.3	50	47	31	28	18	12	8	6	3	1	**204**	43	63	50	24	15	6	2	1	0	0	**204**
	6.3 - 14	27	44	35	34	25	15	11	8	4	1	**204**	33	40	38	44	29	10	6	3	1	0	**204**
	14 - 33	16	28	33	31	30	26	15	12	7	6	**204**	5	33	46	43	31	25	14	4	3	0	**204**
	33 - 66	3	17	44	30	28	32	21	16	7	6	**204**	0	9	41	43	28	36	25	18	4	0	**204**
	66 - 130	2	7	23	27	31	34	28	25	14	12	**203**	0	2	9	35	42	38	35	29	13	1	**204**
	130 - 240	0	9	9	21	27	31	39	28	23	17	**204**	0	0	4	13	43	54	39	24	25	2	**204**
	240 - 490	1	4	6	13	16	21	36	41	36	30	**204**	0	0	0	0	12	29	56	48	40	19	**204**
	490 - 1200	1	1	1	8	16	16	29	32	56	44	**204**	0	0	0	0	1	5	25	66	74	33	**204**
	1200 - 19066	0	0	1	3	3	11	14	35	52	86	**205**	0	0	0	0	0	0	1	10	44	150	**205**
	Total	**204**	**204**	**204**	**204**	**203**	**204**	**204**	**204**	**204**	**204**	**2039**	**204**	**204**	**204**	**204**	**204**	**204**	**204**	**204**	**204**	**205**	**2041**
											Weighted Kappa:	0.51									Weighted Kappa:	0.67
											% of agreement (diagonal only, dark grey cells):	25%									% of agreement (diagonal only, dark grey cells):	32%
											% of agreement (1 decile difference, light grey cells):	32%									% of agreement (1 decile difference, light grey cells):	38%
											% of agreement (2 deciles difference):	21%									% of agreement (2 deciles difference):	22%
											% of agreement (> 2 deciles difference):	22%									% of agreement (> 2 deciles difference):	8%

Italy: 19%, Israel: 11%, Germany: 10%), is shown in Fig. 4. Most participants used more than one communication system during their lifetime use of mobile phones, with 79% having used GSM900 and GSM1800 and 66% having used UMTS2100, while UMTS1800, CDMA1900 and PDC1500 were the least used communication systems, each by only 3%–4% of subjects (Table 3). In addition to mobile phone use, 1460 (72%) subjects reported using DECT phones.

3.4. *Reported laterality and hands-free use*

Less than 4% of subjects reported using Bluetooth, of which 41% reported 'rarely or never' using it, and 15% reported using it 'Less than half of the time'. Thus, considering the values assumed for the various categories for Bluetooth, about 1% of subjects had a reduction of 10% in exposure due to Bluetooth. Hands-free use other than Bluetooth was more prevalent, with 46% reporting it, of which about a third reported using it more than half of the time. Around 3% of DECT phones users reported hands-free use.

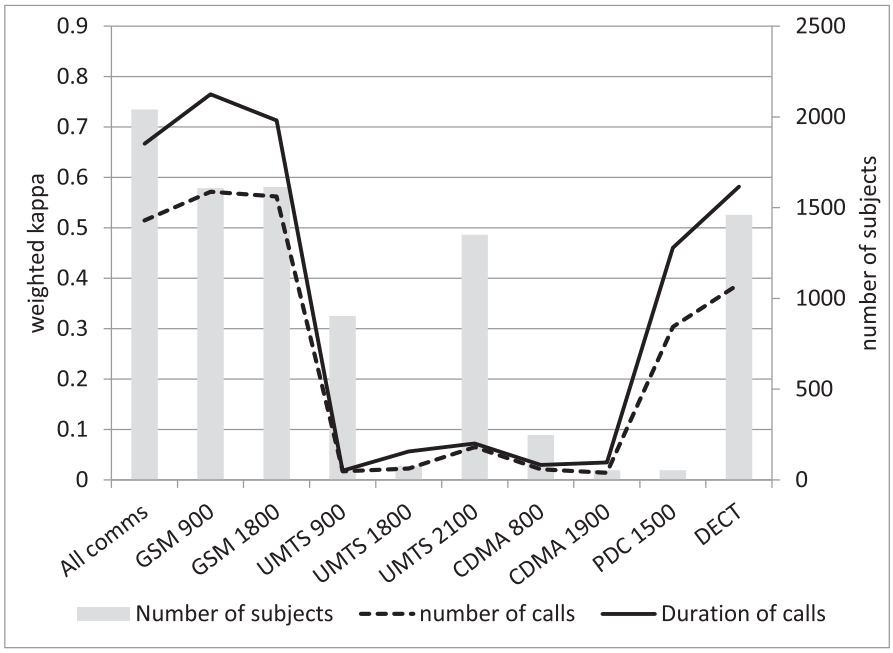

Fig. 6. Weighted kappa (and number of subjects) between CICD and cumulative call time and cumulative number of calls for the various communication systems and total ELF dose.

Over three quarters of subjects reported using the phone on their right (76%) while around 12% reported using it on the left, and 12% on both sides.

Average proportions for left and right laterality are not as strongly dependent on overall laterality reported by subjects, based on the validation studies (Section 2.1.2). Given that dose is effectively a weighted average of exposure with the phone on the left and right of the head, reported laterality does not have a large impact in dose at any given cell. For example, for any given cell in the cartographies chosen as tumour location, RF dose varied by less than 40% when comparing left reported laterality to right one (comparison made for DECT and smartphone for adult brain, for both frequency bands).

3.5. Distribution of RF and ELF cumulative dose across study subjects

Tables 3 and 4 show the summary statistics of the estimated CSE and CICD, respectively, at the COG of the tumour (for controls, dose was estimated at the location of the tumour of the case to which they were matched).

The distributions of RF CSE and ELF CICD were found to be very skewed, overall, and by communication system. Median CSE_s was substantially higher in 2G systems (156 J/kg for GSM 900, 85 J/kg for PDC and somewhat lower, 45 mJ/kg for GSM1800) than 3G (0.09 J/kg–1.24 J/kg). The CSE from DECT phones was similar to that from 3G phones (3.28 J/kg), despite the lack of adaptive power control, reflecting the low values observed in the DECT SAR cartographies (Fig. S4).

Median CICD was highest for GSM phones (very similar for GSM900 and 1800, as ELF ICD does not depend on frequency band); it was an order of magnitude less for PDC, DECT and 3G systems, reflecting the lower ICD in these communication systems compared to GSM.

Tumours with a COG<5 cm from the surface of the brain (N = 115) had a median CSE and CICD of 1238 J/kg and 590 μA·hours/m^2, compared to 133 J/kg and 65 μA·hours/m^2, respectively, for deeper tumours (N = 412).

Table 5 shows the agreement between total CSE and mobile phone use variables (numbers of calls, duration of calls), considering all communication systems together, showing a weighted kappa of 0.55 overall for duration of calls and 0.45 for number of calls. Observed agreement on the diagonal (i.e. proportion of subjects where the RF dose fell in the same decile as duration of calls, for example) was of 24% and 21% respectively. If grouping by quintiles (as done for the main analysis for MOBI-Kids (Castaño-Vinyals 2022)), the kappa values were similar but agreement on the diagonal was higher (45% and 39% for duration and number of calls respectively). For time since start, kappa was 0.24 with an observed agreement on the diagonal of 49%.

The agreement between CSE_s and phone use variables varied by communication system (Fig. 5). It was highest for GSM (0.58 and 0.64 respectively in the 900 MHz and 1800 MHz frequency bands for duration of calls), while the weighted kappa was about 0.24 for duration of calls for DECT phones, 0.35 for PDC and close to 0 for UMTS and CDMA.

Agreement between CICD and wireless phone use variables was slightly higher, with a weighted kappa of 0.67 overall for duration of calls and 0.51 for number of calls (Table 6), and a diagonal agreement of 32% and 25% respectively. The weighted kappa was reasonably high for GSM (0.77 and 0.71 respectively in the 900 and 1800 MHz frequency bands for duration of calls), moderate for DECT (0.58) and PDC (0.46) while close to 0 for UMTS and CDMA (Fig. 6). If grouping by quintiles, the kappa was similar, but agreement was higher (52% and 44% respectively). For time since start, kappa was 0.27 with an observed agreement on the diagonal of 51%.

Correlation between total CSE and total CICD was 0.71 overall, ranging from 0.62 for UMTS1800 to about 0.91 for CDMA 1900, while observed agreement on the diagonal was 39% (Table S5), with a weighted kappa of 0.74 overall, and similar values across all communication systems except for UMTS1800 (0.58) and for CDMA 1900 (0.81).

4. Discussion

This paper presents the algorithm developed to estimate the total RF CSE and ELF CICD at the location of the tumour for the subjects in the MOBI-Kids study. The exposure assessment is an improvement in its scope for such a study in that an attempt was made to consider all characteristics of use, of phones, networks and communication systems that can affect RF and ELF dose to the brain. Median dose estimates reported here provide a general overview of RF and ELF dose for young people in the period from the early 2000 s up to 2015.

An RF dose algorithm has recently been published allowing

estimation of dose to a range of tissues from use of different communication devices (van Wel et al., 2021). For brain dose from mobile phone use at the head, that algorithm in fact uses look-up tables generated from this algorithm (see (Liorni et al., 2020), Table 1), by anatomical region of the brain, not taking into account phone characteristics. None of the other algorithms published to date (Lauer et al., 2013; Liorni et al., 2020; Roser et al., 2015; van Wel et al., 2021) have considered ELF.

This work is particularly relevant since, with the continuing evolution of more energy efficient communication systems over time, duration of use and numbers of calls may not be adequate proxies of RF and ELF dose at a particular location in the brain or other organ, at least when assessed in terms of CSE and CICD. Indeed, the large differences in ICD and SAR for the various mobile communication systems (including APC effects), coupled with the varying proportions of each system's prevalence with time, will have a large impact in the relationship between localised dose and overall cumulative call time. For example, if prevalence were dominated by GSM 1800, dose would be much larger than if it were dominated by UMTS, yet cumulative call time would be the same in both scenarios. Location in the brain (of the tumour), as might be expected, is also a key variable due to the localised nature of dose. This is particularly evident with RF, where dose is mainly focused within a couple of centimetres from the source, and 90% of the reference brain cells are below 10% of the maximum dose across the brain (Table S2). Tumours whose COG were less than 5 cm from the surface of the brain had a median CSE and CICD almost an order of magnitude larger than deeper tumours, highlighting the importance of considering the dose gradient within the brain, even in the case of ELF where the ICD distribution is more diffuse.

Assuming CSE is the gold standard for RF dose and that data grouping is done in deciles, using only duration of calls and number of calls to estimate dose would lead to an exposure misclassification of over 2 deciles for 20% and 28% of subjects respectively, despite moderate overall agreement. As expected, the level of agreement was heavily dependent on communication system – only for 2G systems was there moderate to substantial agreement between duration of use of mobile phones and CSE, and for 2G and DECT for CICD. For example, in this study, duration (or number) of calls was a very poor proxy for exposure to RF (and ELF) for subjects who exclusively used CDMA (e.g. one operator in Canada) and lead to an overestimation of dose. These results illustrate the importance of estimating localised dose in the brain rather than using only mobile phone use history in studies of cancer risk from mobile communication devices use. Notwithstanding, it is difficult to evaluate the lack of agreement for individual communication systems in isolation, as most subjects would have used more than just one communication system during their lifetime. Further, dose is also dependent on location in the brain. In INTERPHONE, observed agreement on the diagonal between total CSE and duration of calls was found to be equal to 34% and the weighted kappa was 0.68 (Cardis et al., 2011b). This is somewhat higher than the values obtained in MOBI-Kids and could be because commercial use of 3G systems was just starting in a few countries at the end of INTERPHONE. In fact, in INTERPHONE, AMPS (a 1G system) was the second most prevalent communication system following GSM800/900 (a 2G system). A similar trend was observed with number of calls (agreement was 27% vs 21% and a weighted kappa of 0.59 vs 0.45 for INTERPHONE and MOBI-Kids respectively).

Despite differences in SAR and ICD distribution across the brain, the correlation between total CSE and total CICD was fairly strong, probably reflecting the overwhelming importance of communication system on both indices, and the dose gradient in the brain. The high correlation and kappa observed suggests that RF dose could be an adequate proxy for ELF dose, and that separate analyses may not be needed.

SAR distributions for the most popular phone categories (bar phone, smart phone, slide phone) were found to be similar upon visual inspection and correlation values, suggesting that phone category has a minor impact in RF dose. Having said that, the diagonal agreement between cartographies suggests that ideally phone category should be considered. The fact that antenna location does not have a large impact on SAR distribution could be because SAR is also affected by other phone components such as the screen. For ELF, differences in ICD between the bar phones and flip/slide phones suggests phone shape may be slightly more important in ELF than RF. In terms of effect of age, the high correlation between the cartographies for the young heads and the adult ones suggests age was not a major determinant of dose distribution (both RF and ELF). However, the fairly low diagonal agreement, coupled with the increase in agreement with age observed in the high frequency band, merits perhaps further investigation.

The validation study performed on volunteers and on a subset of MOBIKIDS study participants in MOBI-Expo (Goedhart et al., 2018) suggests that young people tend to use their phone on both sides of the head, not exclusively on the side of the head where they report using it. Consequently, although laterality was an important exposure determinant at any given time, it was less important when considering cumulative or time-averaged dose estimation.

A major limitation of the algorithm is likely to arise from the uncertainties in the actual communication systems used to make calls and the self-reported usage. Information from operators was sparse and uncertain, including only the start dates of different technologies and the proportions of call traffic using different technologies at one or two points in time. These proportions had to be imputed at different time points by interpolation and information had to be inferred for networks for which no information could be obtained. Even if the interpolations and inferences made were correct, they reflect average conditions in a country for a given year and not the actual conditions in a particular study region at the time a particular call was made. For example, the average proportion of GSM vs UMTS voice traffic from operator data gathered for this study (GSM: 57%, UMTS: 43%) is in line with what was reported by (Roser et al., 2015), which found the proportion to be 55% and 45% respectively (data gathered between 2012 and 2013), suggesting our estimates are likely to be quite representative. Given the very large difference in typical power levels between 2G and 3G systems, the resulting estimates might be expected to be very uncertain. There were also uncertainties related to typical power levels for the various communication systems (for GSM, mean power levels ranged from 35% to 70% depending on country (Vrijheid et al., 2009)), duration of wireless phone use, tumour location and SAR distributions.

Uncertainties in patterns of mobile phone use have been estimated through validation studies (Goedhart et al., 2018; Vrijheid et al., 2009), which showed substantial random error (as opposed to differential systematic error) both in INTERPHONE and MOBI-Kids, plus a tendency to overestimate duration of calls and underestimate number of calls, which varies depending on reported level of use. Overall, the geometric mean ratio of self-reported to recorded was 1.32 and 0.52 for duration and number of calls, respectively (Goedhart et al., 2018).

The main sources of uncertainties in both SAR and ICD distribution include representativeness of head model, representativeness of phone model (e.g. antenna location), transfer of high-resolution modelling to the 1 cm^3 reference brain, phone position and tissue dielectric properties. Estimating the magnitude of these uncertainties is complex and beyond the scope of this paper; however, a simple estimate for the RF and ELF cartographies is presented in Appendix B and suggests an overall fractional uncertainty of about 1 ($k = 1$). Uncertainties in SAR and ICD distribution, and in operator data result in non-differential exposure misclassification which adds noise to dose estimates and could result in underestimation of the association, if there is one, but is unlikely to create a spurious association in the absence of one (Röösli, 2014).With the development of new, more efficient and complex communication systems, EMF dose estimation is likely to be more challenging and subject to larger uncertainties. For example, 5G NR (New Radio) RF exposure is more complex than that of 3G, linked to the enhanced flexibility in how transmission is done. Typical power levels in 5G FR1 (the frequency range currently deployed, 410–7 125 MHz) have been found to be similar to those of 3G systems (Joshi et al., 2020), but the deployment of FR2 (26.5 GHz–48.20 GHz) will introduce larger differences in RF dose distributions than the ones observed in this study,

with much more rapid reduction of dose with increasing depth into the head than at lower frequencies. Thus, even when 2G systems have been phased out, using only duration or number of calls as RF exposure proxies may still result in non-negligible misclassification due to the localised nature of dose distribution in the brain.

5. Conclusion

This paper describes the algorithm constructed to assess the localised RF and ELF dose arising from the use of mobile (cellular) and DECT (cordless) phones in the MOBI-Kids study. The algorithm was based on information on phone use provided by study subjects, on information from operators on prevalence of communication systems as a function of time, on RF and ELF modelling performed as part of the exposure assessment work package (which considered morphological changes due to age), and on validation studies performed within the overall study. ELF and RF dose diminished rapidly with increasing depth, demonstrating location in the brain is an important variable in dose estimation. The agreement between CSE and phone use variables varied by communication system; it was highest for GSM and close to 0 for UMTS and CDMA. Higher agreement was observed between CICD and phone use variables, but agreement was still close to 0 for 3G systems. Analysis of cartographies showed high correlation across phone models and across ages, however diagonal agreement between these cartographies suggest these factors do affect dose distribution to some level and should thus be ideally considered. Overall, the results highlight the importance of considering the effect of communication system and anatomical location in estimating dose and suggests phone use is becoming a poorer exposure proxy as communication systems available for voice calls tend to become more complex with time.

CRediT authorship contribution statement

Carolina Calderon: Methodology, Writing – original draft, Visualization. **Gemma Castaño-Vinyals:** Formal analysis, Visualization, Writing – review & editing. **Myron Maslanyj:** Supervision, Writing – review & editing. **Joe Wiart:** Methodology, Investigation, Software. **Ae-Kyoung Lee:** Methodology, Investigation, Visualization. **Masao Taki:** Methodology, Investigation, Writing – review & editing. **Kanako Wake:** Investigation, Writing – review & editing. **Alex Abert:** Software, Writing – review & editing. **Francesc Badia:** Software, Formal analysis, Visualization, Writing – review & editing. **Abdelhamid Hadjem:** Methodology, Investigation, Writing – review & editing. **Hans Kromhout:** Formal analysis, Writing – review & editing. **Patricia de Llobet:** Formal analysis, Writing – review & editing. **Nadège Varsier:** Methodology, Investigation, Software, Writing – review & editing. **Emmanuelle Conil:** Methodology, Investigation, Software, Writing – review & editing. **Hyung-Do Choi:** Investigation, Writing – review & editing. **Malcolm R. Sim:** Methodology, Writing – review & editing. **Elisabeth Cardis:** Conceptualization, Methodology, Supervision, Project administration, Writing – review & editing.

Declaration of Competing Interest

None of the authors has any personal conflict to declare. Abdelhamid Hadjem, Nadège Varsier, and Emmanuelle Conil were employees of Orange Labs at the time of their involvement with the dosimetry work. Similarly, Joe Wiart was also an employee of Orange Labs prior to 2015. In 2015 Joe Wiart became Ingenieur General des Mines, employed by the Institut Mines-Telecom, a state academic institute. Although they were involved in the modelling and in the development of the dose algorithm as part of the exposure assessment work package, the actual calculation of doses for study subjects was done independently by ISGlobal.

Acknowledgement

The authors would like to acknowledge the work of Anna Peiró (ISGlobal) in running the descriptive analyses in this paper. The authors would also like to acknowledge the MOBI-Kids Consortium.

Funding

Funding for the coordination of the MOBI-Kids study was obtained from the European Commission's Seventh Framework Programme under grant agreements number 226873 and 603794, and from the Spanish Ministry of Science and Innovation (MINECO). In Spain, additional funding was obtained from the Spanish Health Research Fund (FIS) of the National Institute for Health Carlos III, and from the Junta de Andalucía, Consejería de Salud. Proyecto PI-0317-2010. ISGlobal also acknowledges support from the Spanish Ministry of Science, Innovation and Universities through the "Centro de Excelencia Severo Ochoa 2019-2023" Program (CEX2018-000806-S), support from the Generalitat de Catalunya through the CERCA Program and support from the Secretariat of Universities and Research of the Department of Business and Knowledge of the Generalitat of Catalonia through AGAUR (the Catalan Agency for Management of University and Research Grants) (Project 2017 SGR 1487). Australian participation in MOBI-Kids was supported by the Australian National Health and Medical Research Council with a five-year research grant (grant number: 546130). Austrian participation in MOBI-Kids was partly supported by a grant from the Ministry of Science. In Canada, participation in MOBI-Kids was supported by a university-industry partnership grant from the Canadian Institutes of Health Research (CIHR), reference number 110835, with the Canadian Wireless Telecommunications Association (CWTA) serving as the industrial partner. CWTA provides technical information on wireless telecommunications in Canada and facilitates access to billing records from Canadian network operators, but has no involvement in the design, conduct, analysis, or interpretation of the MOBI-KIDS study. French participation was also supported by the French National Agency for Sanitary Safety of Food, Environment and Labour (ANSES, contract FSRF2008-3 and 2013/2/007), French National Cancer Institute (INCa), Pfizer Foundation and League against cancer. The German study centre received additional funding from the Federal Office for Radiation Protection (BfS) under grant number 3609S30010. In Greece, the study was partially supported by the Hellenic Society for Social Pediatrics and Health Promotion, ELKE (Special Account for Research Grants of the National and Kapodistrian University of Athens) and GGET (General Secretariat for Research and Technology). Mobi-Kids India was supported by Board of Research in Nuclear Sciences (BRNS, sanction no: 2013/38/01-BRNS).

Italian participation was partially supported by a Ministry of Health grant (RF-2009-1546284). MOBI-Kids Korea was supported by the ICT R&D program (2017-0-00961 and 2019-0-00102) of MSIT/IITP, Korea. Mobi-Kids Japan was supported by Research on biological electromagnetic environment (Grant Number: JPMI10001) of Ministry of Internal Affairs and Communications Japan. New Zealand participation was supported by the Health Research Council (HRC 12/380) and Cure Kids (grant number 3536). The Netherland's participation in MOBI-KIDS was partly supported by The Netherlands Organisation for Health Research and Development (ZonMw) within the program Electromagnetic Fields and Health Research under grant number 85800001, and by the ODAS foundation, a private foundation supporting activities in the field of pediatric oncology and visual disabilities.

The funding sources had no role in the study design; the collection, analysis, and interpretation of data; the writing of the report; or the decision to submit the article for publication

Appendix A:. Communication systems

This appendix provides a brief overview of the communication

systems considered in the algorithm. Although other communication systems exist, these were not found to be used for voice calls by study subjects, based on their time of usage information and the operator data obtained for their country.

GSM

Global System for Mobile (GSM) Communications is the standard used for second generation (2G) mobile networks in many parts of the world. It was introduced in Europe in the early nineteen nineties and is still widely used for voice calls. It uses Time Division Multiple Access (TDMA), whereby each user is allocated a 0.57 ms timeslot every 4.615 ms. The maximum (peak) power transmitted during GSM calls is 2 W in the 900 MHz band and 1 W for the 1800 MHz band. Considering the discontinuous nature of the transmissions, the maximum time-averaged powers are 250 mW in the 900 MHz band and 125 mW in the 1800 MHz band.

Because transmissions are sent in timeslots as opposed to continuously, the current drawn from the phone battery is pulsed, and has a frequency spectrum with a fundamental peak at 217 Hz with associated harmonics. A small additional 8 Hz signal is also produced due to the multi-frame structure of GSM.

UMTS

Universal Mobile Telecommunications System (UMTS) is the standard used for third generation (3G) mobile networks in Europe and was introduced in the early two thousands. UMTS uses the Wideband Code Division Multiple Access (WCDMA) standard whereby a frequency channel is used simultaneously amongst different users. As a result, UMTS voice frames (10 ms long) are transmitted continuously. Transmission is done at around 900 MHz, 1800 MHz and 2100 MHz for the uplink, with a transmission power of up to 250 mW but typically below 1 mW (Persson et al. 2012).

CDMAOne

First deployed in 1995, CDMAOne is a 2G mobile communication system that, as the name suggests, uses the Code Division Multiple Access (CDMA) standard (similar to that of UMTS) but with a frame duration of 20 ms. Maximum transmitted power is 0.2 W and uplink transmissions were in the 800 MHz band.

PDC

Personal Digital Cellular (PDC) was a 2G telecommunications system exclusively used in Japan between 1993 and 2012 (Korhonen 2014). Maximum transmitted power is 0.267 W for full-rate coding and uplink transmissions were in the 900 MHz and 1500 MHz band. Because it used TDMA like GSM, magnetic fields from mobile phones during PDC calls are pulsed, with a main frequency of 50 Hz or 25 Hz for a frame-to-burst ratio of 3 (full-rate) or 6 (half-rate) respectively.

PHS

Personal Handy-phone System (PHS) is a Japanese communication system standard for cordless phones, introduced in Japan in 1994 (Pandya 2004). Unlike DECT, it allows handover between cells. The system uses a TDMA/TDD system in the 1895–1981 MHz band consisting of a 5 ms frame made of 8 timeslots, 4 for uplink and 4 for downlink, with a maximum output power of 80 mW.

CDMA2000

CDMA2000® represents a family of IMT-2000 (3G) standards providing high-quality voice and broadband data services[3]. Currently, CDMA2000 includes CDMA2000 1X and CDMA2000 EV-DO standards. CDMA2000 1X, deployed in 2000, is used for circuit-switched voice calls, while CDMA2000 EV-DO is used for data. Maximum transmitted power is 0.2 W and uplink transmissions are in the 800 MHz and 1900 MHz bands.

DECT

Digital Enhanced Cordless Telecommunications (DECT) phones were introduced in 1992 to allow for flexible wireless communication in homes and businesses, and by 2002 over 100 million units were being used worldwide (Schiller, 2003). The system uses TDMA like GSM, where each user is allocated a 416.7 μs timeslot every 10 ms (24 timeslots per frame, 12 for uplink and 12 for downlink), resulting in 100 Hz magnetic flux density and harmonics. The maximum peak power of DECT phones is 250 mW (Schiller, 2003), corresponding to a maximum time-averaged power of 10 mW, and transmissions are in the 1800 MHz band.

Appendix B:. Uncertainty budget for ELF cartographies

See Table B1.

Table B1
Uncertainty budget for ICD cartographies. This is a rough estimation on main sources of uncertainty, based on the available information. Not all uncertainty components were able to be quantified. For example, effect of phantom discretisation, 1 cm^3 averaging or mapping onto reference brain is not included in this uncertainty budget.

Source	GSM (bar)	GSM (flip/slide)	DECT	UMTS
Signal variation and instruments[1]	0.06	0.06	0.13	0.25
Loop current (and radius) in model (Variation in magnetic flux density across sample[2])	0.69	0.60	0.49	0.66
Loop position along axis of phone[3]	0.14	0.14	0.14	0.28
Distance between phone and head[4]	0.37	0.37	0.37	0.37
Representativeness of head model[5]	0.3	0.3	0.3	0.3
Conductivity of tissues[6]	0.25	0.25	0.25	0.25
Total (k = 1)	0.89	0.82	0.75	0.93

[1] Taken from uncertainty budget for two-dimensional magnetic flux density measurements.

[2] Combined standard uncertainty of the magnetic flux density two dimensional measurements as well as spectral measurements.

[3] Based on normalised GSM and DECT maps such that the equivalent loop parameters were the same and only loop position along the phone axis differed. The calculation gave a mean uncertainty of < 0.28 across all heads for a 2 cm uncertainty in loop position.

[4] Average uncertainty between 1 cm and 15 cm from the phone (brain position) in magnetic flux density along the axis of the loop due to an uncertainty in loop/phone distance to head of +/- 1 cm.

[5] Based on the data from the 4 different heads used (assumes differences are only due to morphological differences and not age).

[6] (Gabriel et al. 1996b) reported a variation in tissue conductivities at low frequencies of 15–25% due to inhomogeneity of tissues. Repeatability of measurements was 1%. Uncertainty due to anisotropy of tissues not included.

[3] https://www.cdg.org/technology/cdma2000.asp.

Appendix C. Supplementary material

Supplementary data to this article can be found online at https://doi.org/10.1016/j.envint.2022.107189.

References

1999/5/EC, D. Directive 1999/5/EC of the European Parliament and of the Council of 9 March 1999 on radio equipment and telecommunications terminal equipment and the mutual recognition of their conformity. European Parliament, Council of the European Union 1999; 2014/53/EU, R. Radio Equipment directive (RED). In: Commission E., ed; 2014.

Calderón, C., Addison, D., Mee, T., Findlay, R., Maslanyj, M., Conil, E., Kromhout, H., Lee, A.-K., Sim, M.R., Taki, M., Varsier, N., Wiart, J., Cardis, E., 2014. Assessment of extremely low frequency magnetic field exposure from GSM mobile phones. Bioelectromagnetics 35 (3), 210–221.

Calderón, C., Ichikawa, H., Taki, M., Wake, K., Addison, D., Mee, T., Maslanyj, M., Kromhout, H., Lee, A.-K., Sim, M.R., Wiart, J., Cardis, E., 2017. ELF exposure from mobile and cordless phones for the epidemiological MOBI-Kids study. Environ. Int. 101, 59–69.

Cardillo, G., 2007. Cohens kappa: compute the Cohen's kappa ratio on a 2x2 matrix. (https://www.mathworks.com/matlabcentral/fileexchange/15365-cohen-s-kappa). MATLAB Central File Exchange. Retrieved July, 2015.

Cardis, E., Armstrong, B.K., Bowman, J.D., Giles, G.G., Hours, M., Krewski, D., McBride, M., Parent, M.E., Sadetzki, S., Woodward, A., Brown, J., Chetrit, A., Figuerola, J., Hoffmann, C., Jarus-Hakak, A., Montestruq, L., Nadon, L., Richardson, L., Villegas, R., Vrijheid, M., 2011a. Risk of brain tumours in relation to estimated RF dose from mobile phones: results from five Interphone countries. Occup. Environ. Med. 68 (9), 631–640.

Cardis, E., Varsier, N., Bowman, J.D., Deltour, I., Figuerola, J., Mann, S., Moissonnier, M., Taki, M., Vecchia, P., Villegas, R., Vrijheid, M., Wake, K., Wiart, J., 2011b. Estimation of RF energy absorbed in the brain from mobile phones in the Interphone Study. Occup. Environ. Med. 68 (9), 686–693.

Castaño-Vinyals, G., Sadetzki, S., Vermeulen, R., Momoli, F., Kundi, M., Merletti, F., Maslanyj, M., Calderon, C., Wiart, J., Lee, A.-K., Taki, M., Sim, M., Armstrong, B., Benke, G., Schattner, R., Hutter, H.-P., Krewski, D., Mohipp, C., Ritvo, P., Spinelli, J., Lacour, B., Remen, T., Radon, K., Weinmann, T., Petridou, E.T., Moschovi, M., Pourtsidis, A., Oikonomou, K., Kanavidis, P., Bouka, E., Dikshit, R., Nagrani, R., Chetrit, A., Bruchim, R., Maule, M., Migliore, E., Filippini, G., Miligi, L., Mattioli, S., Kojimahara, N., Yamaguchi, N., Ha, M., Choi, K., Kromhout, H., Goedhart, G., 't Mannetje, A., Eng, A., Langer, C.E., Alguacil, J., Aragonés, N., Morales-Suárez-Varela, M., Badia, F., Albert, A., Carretero, G., Cardis, E., 2022. Wireless phone use in childhood and adolescence and neuroepithelial brain tumours: Results from the international MOBI-Kids study. Environ. Int. 160, 107069.

Christ, A., Kainz, W., Hahn, E.G., Honegger, K., Zefferer, M., Neufeld, E., Rascher, W., Janka, R., Bautz, W., Chen, J.i., Kiefer, B., Schmitt, P., Hollenbach, H.-P., Shen, J., Oberle, M., Szczerba, D., Kam, A., Guag, J.W., Kuster, N., 2010. The Virtual Family–development of surface-based anatomical models of two adults and two children for dosimetric simulations. Phys. Med. Biol. 55 (2), N23–N38.

Cohen, J., 1960. A coefficient of agreement for nominal scales. Educational Psychol. Measurement 20 (1), 37–46.

Cohen, J., 1968. Weighted kappa: nominal scale agreement with provision for scaled disagreement or partial credit. Psychol. Bull. 70, 213–220.

Courchesne, E., Chisum, H.J., Townsend, J., Cowles, A., Covington, J., Egaas, B., Harwood, M., Hinds, S., Press, G.A., 2000. Normal Brain Development and Aging: Quantitative Analysis at in Vivo MR Imaging in Healthy Volunteers. 216 672-682.

Dimbylow, P., 1995. The development of realistic voxel phantoms for electromagnetic field dosimetry. Voxel phantom development. Proceedings of an international workshop: National Radiological Protection Board.

Gabriel, C., Gabriel, S., Corthout, E., 1996a. The dielectric properties of biological tissues: I. Literature survey. Phys. Med. Biol. 41 (11), 2231–2249.

Gabriel, S., Lau, R.W., Gabriel, C., 1996b. The dielectric properties of biological tissues: II. Measurements in the frequency range 10 Hz to 20 GHz. Phys. Med. Biol. 41 (11), 2251–2269.

Gati, A., Hadjem, A., Wong, M.-F., Wiart, J., 2009. Exposure induced by WCDMA mobiles phones in operating networks. IEEE Trans. Wireless Commun. 8 (12), 5723–5727.

Ghanmi, A., 2013. Analyse de l'exposition aux ondes électromagnétiques des enfants dans le cadre des nouveaux usages et nouveaux réseaux. Électronique, optronique et systèmes. Université Marne la Vallée.

Ghanmi, A., Varsier, N., Hadjem, A., Conil, E., Picon, O., Wiart, J., 2014. Analysis of the influence of handset phone position on RF exposure of brain tissue. Bioelectromagnetics 35 (8), 568–579.

Giedd, J.N., Clasen, L.S., Lenroot, R., Greenstein, D., Wallace, G.L., Ordaz, S., Molloy, E. A., Blumenthal, J.D., Tossell, J.W., Stayer, C., Samango-Sprouse, C.A., Shen, D., Davatzikos, C., Merke, D., Chrousos, G.P., 2006. Puberty-related influences on brain development. Mol. Cell. Endocrinol. 254–255, 154–162.

Goedhart, G., van Wel, L., Langer, C.E., de Llobet Viladoms, P., Wiart, J., Hours, M., Kromhout, H., Benke, G., Bouka, E., Bruchim, R., Choi, K.-H., Eng, A., Ha, M., Huss, A., Kiyohara, K., Kojimahara, N., Krewski, D., Lacour, B., 't Mannetje, A., Maule, M., Migliore, E., Mohipp, C., Momoli, F., Petridou, E.T., Radon, K., Remen, T., Sadetzki, S., Sim, M., Weinmann, T., Cardis, E., Vrijheid, M., Vermeulen, R., 2018. Recall of mobile phone usage and laterality in young people: The multinational Mobi-Expo study. Environ. Res. 165, 150–157.

Gosselin, M.-C., Kühn, S., Kuster, N., 2013. Experimental and numerical assessment of low-frequency current distributions from UMTS and GSM mobile phones. Phys. Med. Biol. 58 (23), 8339–8357.

Gosselin, M.-C., Neufeld, E., Moser, H., Huber, E., Farcito, S., Gerber, L., Jedensjö, M., Hilber, I., Gennaro, F.D., Lloyd, B., Cherubini, E., Szczerba, D., Kainz, W., Kuster, N., 2014. Development of a new generation of high-resolution anatomical models for medical device evaluation: the Virtual Population 3.0. Phys. Med. Biol. 59 (18), 5287–5303.

Han, M., Lee, A.-K., Choi, H.-D., Jung, Y.W., Park, J.S., 2018. Averaged head phantoms from magnetic resonance images of Korean children and young adults. Phys. Med. Biol. 63 (3), 035003.

IEC-62209-1528, 2020. IEEE/IEC 62209-1528-2020 - IEC/IEEE International Standard - Measurement procedure for the assessment of specific absorption rate of human exposure to radio frequency fields from hand-held and body-mounted wireless communication devices – Part 1528: Human models, instrumentation, and procedures (Frequency range of 4 MHz to 10 GHz). IEC/IEEE International Standard.

Joshi, P., Ghasemifard, F., Colombi, D., Törnevik, C., 2020. Actual output power levels of user equipment in 5G commercial networks and implications on realistic RF EMF exposure assessment. IEEE Access 8, 204068–204075.

Kelsh, M.A., Shum, M., Sheppard, A.R., Mcneely, M., Kuster, N., Lau, E., Weidling, R., Fordyce, T., Kühn, S., Sulser, C., 2011. Measured radiofrequency exposure during various mobile-phone use scenarios. J. Eposure Sci. Environ. Epidemiol. 21 (4), 343–354.

Korhonen, J., 2014. Introduction to 4G Mobile Communications edˆeds. Artech House.

Lauer, O., Frei, P., Gosselin, M.-C., Joseph, W., Röösli, M., Fröhlich, J., 2013. Combining near- and far-field exposure for an organ-specific and whole-body RF-EMF proxy for epidemiological research: a reference case. Bioelectromagnetics 34 (5), 366–374.

Lee, A.-K., Byun, J.-K., Park, J.S., Choi, H.-D., Yun, J., 2009. Development of 7-year-old Korean child model for computational dosimetry. ETRI J. 31 (2), 237–239. https://doi.org/10.4218/etrij.09.0208.0342.

Lee, A.-K., Choi, W.Y., Chung, M.S., Choi, H.-d., Choi, J.-I., 2006. Development of Korean male body model for computational dosimetry. ETRI J. 28 (1), 107–110. https://doi.org/10.4218/etrij.06.0205.0024|.

Lee, A.-K., Hong, S.-E., Kwon, J.-H., Choi, H.-D., Cardis, E., 2017. Mobile phone types and SAR characteristics of the human brain. Phys. Med. Biol. 62 (7), 2741–2761.

Lee, A.-K., Yoon, Y., Lee, S., Lee, B., Hong, S.-E., Choi, H.-D., Cardis, E., 2016. Numerical implementation of representative mobile phone models for epidemiological studies. J. Electromagnetic Eng. Sci. 16 (2), 87–99. https://doi.org/10.5515/JKIEES.2016.16.2.87.

Lee, A.-K., Hong, S.-E., Taki, M., Wake, K., Choi, H.-D., 2018. Comparison of different SAR limits in SAM phantom for mobile phone exposure In: 2018 Asia-Pacific Microwave Conference (APMC). IEEE. https://doi.org/10.23919/APMC.2018.8617343. https://ieeexplore.ieee.org/document/8617343.

Lee, A.-K., Choi, H.-D., 2012. Determining the influence of Korean population variation on whole-body average SAR. Phys. Med. Biol. 57 (9), 2709–2725.

Lee, A.-K., Choi, H.-D., 2020. Brain EM exposure for voice calls of mobile phones in wireless communication environment of Seoul, Korea. IEEE Access 8, 163176–163185. https://doi.org/10.1109/ACCESS.2020.3020831.

Lee, A.-K., Park, J.S., Hong, S.-E., Taki, M., Wake, K., Wiart, J., Choi, H.-D., 2019. Brain SAR of average male Korean child to adult models for mobile phone exposure assessment. Phys. Med. Biol. 64 (4), 045004.

Liorni, I., Capstick, M., van Wel, L., Wiart, J., Joseph, W., Cardis, E., Guxens, M., Vermeulen, R., Thielens, A., 2020. Evaluation of specific absorption rate in the far-field, near-to-far field and near-field regions for integrative radiofrequency exposure assessment. Radiat. Prot. Dosim. 190, 459–472.

Mahfouz, Z., Gati, A., Lautru, D., Wiart, J., Hanna, V.F., 2012. SAR assessment and analysis of cumulative body exposure to multi transmitters from a mobile phone. 2012 IEEE Topical Conference on Biomedical Wireless Technologies, Networks, and Sensing Systems (BioWireleSS).

Nagaoka, T., Watanabe, S., Sakurai, K., Kunieda, E., Watanabe, S., Taki, M., Yamanaka, Y., 2004. Development of realistic high-resolution whole-body voxel models of Japanese adult males and females of average height and weight, and application of models to radio-frequency electromagnetic-field dosimetry. Phys. Med. Biol. 49 (1), 1–15.

Orcutt, N., Gandhi, O.P., 1988. A 3-D impedance method to calculate power deposition in biological bodies subjected to time varying magnetic fields. IEEE Trans. Biomed. Eng. 35 (8), 577–583.

Pandya, R., 2004. Mobile and Personal Communication Services and Systems. Wiley.

Persson, T., Törnevik, C., Larsson, L.-E., Lovén, J., 2012. Output power distributions of terminals in a 3G mobile communication network. Bioelectromagnetics 33 (4), 320–325.

Röösli, M. (Ed.), 2014. Epidemiology of Electromagnetic Fields. CRC Press.

Roser, K., Schoeni, A., Bürgi, A., Röösli, M., 2015. Development of an RF-EMF exposure surrogate for epidemiologic research. Int. J. Environ. Res. Public Health 12, 5634–5656. https://doi.org/10.3390/ijerph120505634.

Sadetzki, S., Langer, C.E., Bruchim, R., Kundi, M., Merletti, F., Vermeulen, R., Kromhout, H., Lee, A.-K., Maslanyj, M., Sim, M.R., Taki, M., Wiart, J., Armstrong, B., Milne, E., Benke, G., Schattner, R., Hutter, H.P., Woehrer, A., Krewski, D., Mohipp, C., Momoli, F., Ritvo, P., Spinelli, J., Lacour, B., Delmas, D., Remen, T., Radon, K., Weinmann, T., Klostermann, S., Heinrich, S., Petridou, E., Bouka, E., Panagopoulou, P., Dikshit, R., Nagrani, R., Even-Nir, H., Chetrit, A., Maule, M., Migliore, E., Filippini, G., Miligi, L., Mattioli, S., Yamaguchi, N., Kojimahara, N., Ha, M., Choi, K.-H., Mannetje, A., Eng, A., Woodward, A., Carretero, G., Alguacil, J., Aragones, N., Suare-Varela, M.M., Goedhart, G., Schouten-van Meeteren, A.A., Reedijk, A.A., Cardis, E., 2014. The MOBI-Kids study protocol: challenges in assessing childhood and adolescent exposure to electromagnetic fields from wireless

telecommunication technologies and possible association with brain tumor risk. Front. Public Health 2, 124. https://doi.org/10.3389/fpubh.2014.00124.
Schiller, J.H., 2003. Mobile Communications edˆeds: Addison-Wesley.
Stüber, G.L. (Ed.), 2017. Principles of Mobile Communication. Springer International Publishing, Cham.
Taki, M.; Personal communication.
van Wel, L., Liorni, I., Huss, A., Thielens, A., Wiart, J., Joseph, W., Röösli, M., Foerster, M., Massardier-Pilonchery, A., Capstick, M., Cardis, E., Vermeulen, R., 2021. Radio-frequency electromagnetic field exposure and contribution of sources in the general population: an organ-specific integrative exposure assessment. J. Expo Sci. Environ. Epidemiol. 31 (6), 999–1007.
Vrijheid, M., Mann, S., Vecchia, P., Wiart, J., Taki, M., Ardoino, L., Armstrong, B.K., Auvinen, A., Bedard, D., Berg-Beckhoff, G., Brown, J., Chetrit, A., Collatz-Christensen, H., Combalot, E., Cook, A., Deltour, I., Feychting, M., Giles, G.G., Hepworth, S.J., Hours, M., Iavarone, I., Johansen, C., Krewski, D., Kurttio, P., Lagorio, S., Lonn, S., McBride, M., Montestrucq, L., Parslow, R.C., Sadetzki, S., Schuz, J., Tynes, T., Woodward, A., Cardis, E., 2009. Determinants of mobile phone output power in a multinational study: implications for exposure assessment. Occup. Environ. Med. 66 (10), 664–671.
Wake, K., Watanabe, Taki., 2005. General Conference of the Institute of Electronics, Information and Communication Engineers (IEICE).
Wang, J., Fujiwara, O., Watanabe, S., 2006. Approximation of aging effect on dielectric tissue properties for SAR assessment of mobile telephones. IEEE Trans. Electromagn. Compat. 48 (2), 408–413.
Wiart, J., Dale, C., Bosisio, A.V., Cornec, A.L., 2000. Analysis of the influence of the power control and discontinuous transmission on RF exposure with GSM mobile phones. IEEE Trans. Electromagn. Compat. 42, 376–385.
Wiart, J., Hadjem, A., Varsier, N., Bloch, I., Person, C., Gati, A. and Conil, E., 2013. Comparative Analysis of the Human Exposure induced by RF mobile phones and base stations. In: International Symposium on Electromagnetic Theory (EMTS 2013). Hiroshima, Japan.
Wiart, J., Hadjem, A., Varsier, N., Conil, E., 2011. Numerical dosimetry dedicated to children RF exposure. Prog. Biophys. Mol. Biol. 107 (3), 421–427.
Wiart, J., Hadjem, A., Wong, M.F., Bloch, I., 2008. Analysis of RF exposure in the head tissues of children and adults. Phys. Med. Biol. 53 (13), 3681–3695.
Wu, T., Tan, L., Shao, Q., Zhang, C., Zhao, C., Li, Y., Conil, E., Hadjem, A., Wiart, J., Lu, B., Xiao, L.i., Wang, N., Xie, Y.i., Zhang, S., 2011. Chinese adult anatomical models and the application in evaluation of RF exposures. Phys. Med. Biol. 56 (7), 2075–2089.
Xu, X.G., Eckerman, K.F., 2009. Handbook of anatomical models for radiation dosimetry. CRC Press.